Soluble precipitable porphyrins for use in targeted molecular brachytherapy†

Zhen Yao, K. Eszter Borbas and Jonathan S. Lindsey*

Received (in Gainesville, FL, USA) 13th September 2007, Accepted 23rd October 2007
First published as an Advance Article on the web 2nd November 2007
DOI: 10.1039/b714127k

In a new therapy that aims to concentrate and immobilize therapeutic radionuclides in nanoscale assemblies within solid tumors, a soluble precipitable reagent (SPR) is administered as the radionuclide carrier and is converted to non-diffusible precipitate by an enzyme located in tumor tissues. To meet the objective of such an SPR, we have prepared and examined a class of porphyrin–alkyldiphosphates that are soluble in aqueous solution and that are rendered insoluble upon removal of the two phosphate groups. The porphyrins examined herein are of the *trans*-AB architecture wherein the substituents are a bis(dihydroxyphosphoryloxy)alkyl group and a phenyl (or *p*-bromophenyl) group. Provisions for later incorporation of radionuclides have been established by preparation of the analogous copper chelate or the *meso*-iodo free-base porphyrin. Altogether, four porphyrins bearing a bis(dihydroxyphosphoryloxy)alkyl group were examined and found to exhibit satisfactory solubility in water (>1 mM). Dephosphorylation reactions have been carried out *in vitro* using the enzyme shrimp alkaline phosphatase. In each case, enzyme-induced precipitation was observed. The soluble-to-insoluble conversion has been examined by visual inspection, absorption spectroscopy, electrospray ionization mass spectrometry, and nephelometry using non-radiolabeled porphyrins.

Introduction

Fundamentally new approaches are urgently needed for therapeutic treatment of cancer, which has surpassed heart disease as the leading cause of death in the United States for persons younger than 85.[1] Of all types of cancers, solid tumors are now estimated to account for more than 80% of all incidents of cancer diagnosis and death.[2] Surgery and radiation therapy may be successful for treating localized solid tumors, but not for metastases. Chemotherapy of metastasized tumors is limited due to the heterogeneity of tumors, the plasticity of cancer cells, and the imperfect differentiation between healthy and tumor tissue.[3,4] Although systemic agents are essential for the treatment of metastatic cancer, the occurrence of adverse side effects typically limits the maximum dose of the anti-cancer agent that can be administered.

Diverse targeted cancer therapies (*e.g.*, antibodies, macromolecules, nanoparticles, viral vectors)[5–12] have been examined in an effort to increase the therapeutic index (*i.e.*, selectively deliver the therapeutic agents to the tumor location and thereby diminish the systemic cytotoxicity). Despite tremendous effort, however, the various targeted methods developed to date have generally not been successful for treating disseminated cancers. There appear to be three universal obstacles to further progress of targeted cancer therapies: (1) the current therapeutic agents only target a subset of cancer cells in the intrinsically heterogeneous tumor, whereupon the remaining cell types give rise to resistant colonies;[3] (2) the agents also kill normal cells because of non-exclusive selectivity toward cancer cells; and (3) the agents are not potent enough to kill resistant cancer cells or to overcome the ability of cancer cells to adapt to the agents and become resistant.[4] Note also that a combination of multiple chemotherapeutic drugs, each having distinct chemical structure and each blocking a different biochemical pathway, has not significantly prolonged the survival of cancer patients.[13]

A decade ago, a fundamentally new strategy to treat cancer was proposed by Rose.[14–16] The proposed approach mimics the treatment of thyroid cancer with radioiodide. Compared to other types of cancer, thyroid cancer often can be successfully treated.[17] The thyroid naturally concentrates iodide from body fluids; therefore, the administration of radioiodide results in localization of most of the radiation damage inside the thyroid with little systemic damage. Similarly, the goal of Rose's method is to concentrate radionuclides inside tumors (both primary and metastatic tumors) by systemic administration of a set of therapeutic agents, including both non-radiolabeled agents and radiolabeled agents.

To selectively deliver the radiolabeled materials to tumors and maintain the radiation within a well-defined area, Rose's method employs a multi-step regimen that employs the following four reagents in successive steps:

(1) A soluble reagent bearing a cancer-targeting agent and an enzyme-binding moiety is administered (Step-1 reagent).

Department of Chemistry, North Carolina State University, Raleigh, NC 27695-8204, USA. E-mail: jlindsey@ncsu.edu; Fax: 1 919 513 2830; Tel: 1 919 515 6406

† Electronic supplementary information (ESI) available: ESI-MS data for enzymatically treated samples of water-soluble porphyrins. See DOI: 10.1039/b714127k

Such a reagent is endocytosed preferentially but not exclusively in cancer cells owing to the presence of the cancer-targeting agent. Upon endocytosis, a chemical conversion occurs that results in the formation of a precipitate. The precipitate, termed 'platform', constitutes a nanoscale architecture that is non-diffusible and that contains the enzyme-binding moiety in an accessible state (*vide infra*). Due to the capacity for soluble-to-insoluble conversion, this reagent is a type of soluble precipitable reagent (SPR), in particular a Step-1 SPR.

(2) A low dose of a cytotoxic drug (*e.g.*, doxorubicin) is administered (Step-2 reagent), which kills a small fraction of the super-sensitive cancer cells. The subsequent cell lysis releases some of the platform to the extracellular medium. The normal cells are unaffected by the low dose of the cytotoxic drug, hence the platform is retained inside such cells.

(3) An enzyme conjugate, which is not naturally present or accessible in the extracellular area, is administered (Step-3 reagent). The enzyme attaches covalently to the platform (released into the extracellular medium in step 2) *via* the enzyme-binding moiety, thereby localizing and immobilizing the enzyme in the tumor. The Step-3 reagent is cell-impermeable to preclude binding to the platform located inside cells in normal tissues (as well as un-lysed cancer cells). It is known that enzymes in aggregated or precipitated forms can maintain a high level of activity.[18]

(4) A radiolabeled SPR, which precipitates upon action of the enzyme attached to the platform in step 3, is administered (Step-4 reagent). The radiolabeled (and immobile) precipitate generated by the Step-4 SPR forms a radiation field inside the tumors, destroying potentially every cancer cell within the effective radius of the radiation.

One term for this four-step procedure is "selectively targeted amplified radiotherapy" (STAR),[19] which denotes the following features: (1) a combination of two "imperfect" targeting steps that causes localization of the therapeutic agent near the most sensitive cancer cells; (2) generation of a strong radiation field to destroy every cell in a given micro-region; and (3) amplified localization and immobilization of radiotherapy sources in the tumor. Although the concept of the STAR method was inspired by the treatment for thyroid cancer, the overall therapeutic effect has great similarity to that of brachytherapy,[20] wherein radioactive seeds, typically small capsules enclosing radioactive materials, are surgically implanted in or near tumor tissues. The radiolabeled precipitate formed in the STAR method is comparable in principle to the radioactive seed in traditional brachytherapy, but has the advantages of (1) nanoscale assembly *in situ*, (2) targeting of both primary and metastatic tumor tissues; (3) separation of the targeting and therapeutic steps, and (4) administration without surgery. Therefore, Rose's method constitutes a "targeted molecular brachytherapy", given the ability to selectively deposit radiation sources inside the tumor and cause micro-regional destruction of surrounding cancer cells.

The cornerstone of the STAR method is a novel class of soluble chemical compounds particularly the Step-1 SPR, the Step-4 SPR, and the enzyme conjugate (Step-3 reagent). The core of a SPR is an inherently insoluble entity that is rendered soluble by the attachment of enzymatically cleavable solubilizing groups, such as phosphates,[21] sulfates,[22] or sugars[23] (*e.g.*, glucosides or galactosides). One SPR presently under development[24] (at Oncologic, Inc., a company founded by Rose) is designed around derivatives of an indoxyl glycoside. Such a chemical structure was chosen because mammalian lysosomes contain enzymes that will cleave the sugar to form the corresponding indoxyl. The indoxyl undergoes oxidative (aerobic) dimerization to give insoluble indigo (Scheme 1). With appropriate prior chemical modification, the indigo precipitate provides the platform for subsequent localization of radioactive material. *In vitro* studies showed the accumulation of indigo (blue) inside the tumor cells, and the presence of a binding handle (*e.g.*, a Loracarbef moiety) on the precipitate was demonstrated by an immunoassay.[19] These preliminary results prove the viability of the strategy on which the STAR method is established.

Although the full STAR method has not yet been demonstrated, in recent years, other approaches have been developed that embody selected steps of the STAR method. Pretargeted radioimmunotherapy employs an antibody bearing avidin to target the cancer, followed by administration of a radiolabeled biotin derivative.[6,7,9,10] This approach suffers from lack of immobilization of the antibody in the tumor, and rapid clearance of the antibodies in the kidney.[25] Enzyme-mediated cancer therapy employs a water-soluble radiolabeled prodrug that is hydrolyzed enzymatically *in vivo* to give a water-insoluble compound; the group to be cleaved is the substrate of an enzyme that is overexpressed extracellularly by tumor cells.[26] Thus, the water-soluble radiolabeled prodrug is in essence a Step-4 SPR. The one example that has been demonstrated to date is a radiolabeled iodo-quinazolinone that bears a phosphoryloxy group; dephosphorylation results in formation of a radiolabeled precipitate.[27] The design of a Step-4 SPR also has some commonality with certain reagents for enzyme histochemical staining, wherein a soluble chromogen (*e.g.*, diaminobenzidine, or even indoxyl phosphate) is converted to an insoluble form.[28]

In this paper, we describe our work concerning the development of porphyrin-based SPRs. There are multiple reasons for choosing porphyrins as the backbone of an SPR: (1) the extensive knowledge-base concerning water-soluble

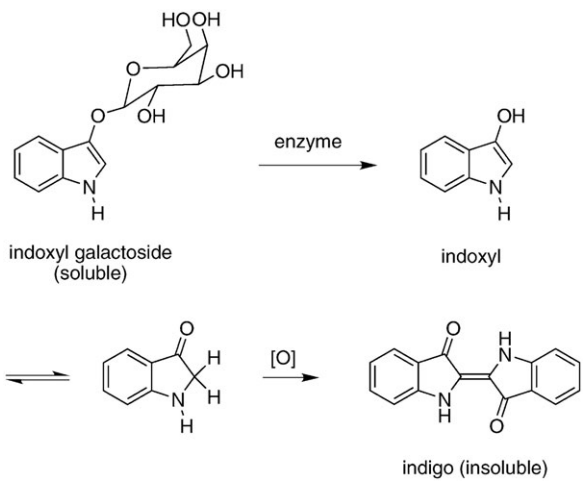

Scheme 1

porphyrins[29] and aggregation of porphyrinic compounds;[30] (2) rational synthetic methods for preparing porphyrins enable introduction of up to four functional groups in distinct patterns;[31–35] (3) the robustness of the synthetic porphyrin macrocycle in biological systems; (4) low molecular weight (<1000 μ); and (5) the ability to use porphyrins as carriers for diverse radionuclides encompassing radioiodine and radioactive metals.

Our initial focus concerns the design and synthesis of a water-soluble porphyrin that serves as a Step-4 SPR. Solubilization is achieved by the attachment of a symmetrically branched alkyl chain equipped with phosphate groups at the termini ("swallowtail" motif).[36] The essential soluble-to-insoluble conversion has been investigated *via* various spectroscopic methods. Synthetic routes to a porphyrin-based Step-4 SPR bearing iodo groups or a copper chelate were investigated, thereby providing the foundation for later preparation of radiolabeled analogues (*e.g.*, containing ^{131}I or ^{64}Cu). Taken together, this work provides the foundation for the development of a new class of molecules for use in targeted molecular brachytherapy.

Results and discussion

1 Molecular design

The structural motifs for a Step-4 reagent include (1) the ability to undergo conversion from soluble-to-insoluble forms, (2) ability to carry radionuclides, and (3) formation of a non-diffusible precipitate.

Low aqueous solubility is a common problem with porphyrins because such planar aromatic compounds tend to aggregate upon π–π interactions among the aromatic rings.[29] Low solubility in aqueous media is an excellent property for the product of the soluble-to-insoluble conversion of an SPR, but first the porphyrin must be rendered soluble in aqueous media. Substituted phenyl groups such as 3,5-di-*tert*-butylphenyl and mesityl groups impart higher organic solubility to the porphyrin than the phenyl group.[36] A likely explanation is that the alkyl moieties on the *meso*-phenyl groups shield the space above and below the macrocycle, and thus suppress π–π interactions. Another type of *meso*-substituent that solubilizes porphyrins by the same shielding strategy is a symmetrically branched alkyl group (*i.e.*, swallowtail, Fig. 1).[36,37] Taking advantage of the facial encumbrance of the swallowtail group, the swallowtail design was modified to accommodate polar moieties such as phosphate or phosphonate groups at the terminus of each alkyl group. The projection of polar groups over both faces of the porphyrin macrocycle was expected to render the molecules highly water-soluble.

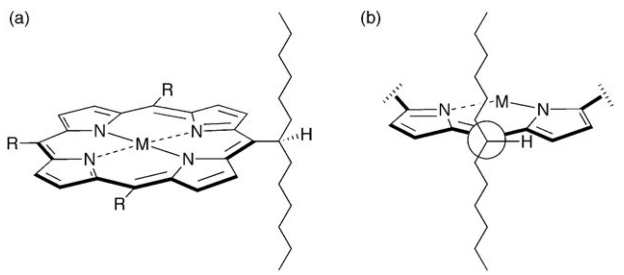

Fig. 1 A porphyrin bearing a meso-swallowtail substituent. (a) Side view; (b) Newman projection. Adapted from ref. 36.

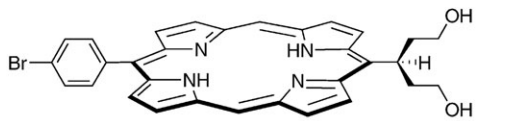

P1-(OH)$_2$

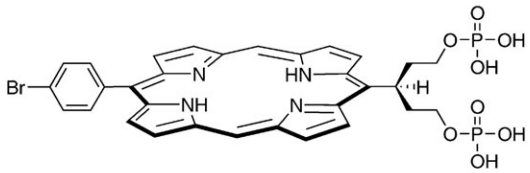

P1-(PO$_4$)$_2$

Chart 1

Diphosphate-derivatized swallowtail porphyrins in a *trans*-AB design were prepared in a rational synthesis.[38] A *trans*-AB-porphyrin bears substituents only at the 5- and 15-positions, resulting in a compact design that is well suited for biological applications. Indeed, the free-base porphyrin **P1-(PO$_4$)$_2$** (5-(4-bromophenyl)-15-[1,5-bis(dihydroxyphosphoryloxy)pent-3-yl]porphyrin), which bears one swallowtail substituent, one derivatizable group (4-bromophenyl), and no substituents at the flanking *meso* positions, displays excellent solubility in water (Chart 1).

During the development of the water-solubilizing swallowtail motifs, it was observed that the presence of a central zinc atom in the porphyrin–alkyldiphosphates yielded a precipitate in protic solvents within a short time. The precipitate was found to be the poorly aqueous-soluble dihydroxyporphyrin **ZnP1-(OH)$_2$**. The facile **ZnP1-(PO$_4$)$_2$** → **ZnP1-(OH)$_2$** conversion was ascribed to coordination of one of the phosphate oxygens to the zinc, followed by nucleophilic attack by a solvent molecule (Scheme 2). We hypothesized that a similar soluble-to-insoluble transformation could be achieved upon treatment of the free-base porphyrin with a phosphatase enzyme. Similarly, a metalloporphyrin wherein the metal does not support apical binding (*e.g.*, copper) could be used.

A further advantage of using a *trans*-AB porphyrin as the SPR is the availability of two *meso* positions for radioiodination, and the possibility of metalation with a radioactive metal to give the metalloporphyrin. In this regard, a number of radiolabeled porphyrins have been employed both in diagnosis and in therapy.[39] Representative radiometals for inclusion as the centrally coordinated metal in a metalloporphyrin include the following: ^{51}Mn (ref. 40), ^{54}Mn (ref. 41), ^{57}Co (ref. 42), ^{58}Co (ref. 43), ^{64}Cu (refs. 44 and 45), ^{65}Zn (ref. 43), ^{67}Cu (refs. 44 and 46), ^{67}Ga (ref. 47), ^{90}Y (refs. 48 and 49), ^{99m}Tc (ref 50), ^{109}Pd (refs. 45, 51 and 52), ^{111}In (refs. 47 and 53), ^{166}Ho (ref. 48), and ^{169}Yb (ref. 49). The radiolabel ^{123}I (ref. 54) or ^{18}F (ref. 55) has been substituted on the aryl ring of a *meso*-tetraarylporphyrin (but not the *meso*-position itself). While already quite diverse, other radiolabeled (metallo)porphyrins also can be envisaged.

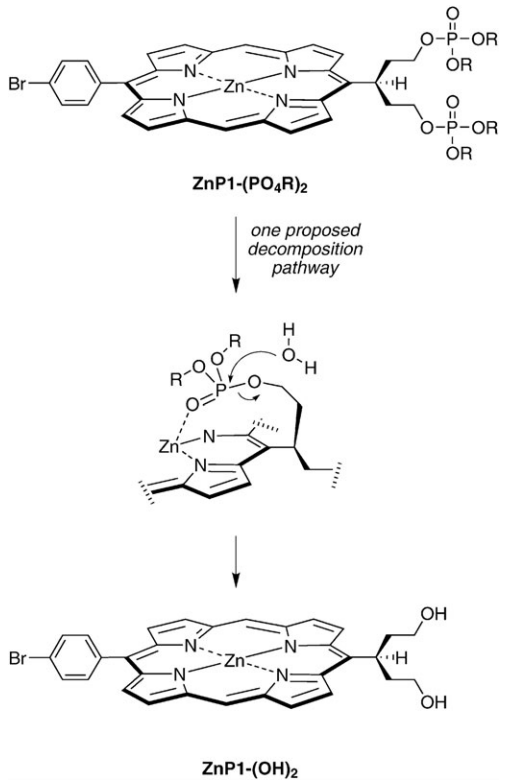

Scheme 2

2 Synthesis

A. Porphyrin synthesis. The target porphyrins are of the *trans*-AB type, bearing the swallowtail motif and an aromatic substituent at the 5- and 15- (*meso*) positions. This design exploits synthetic accessibility and employs the minimum number of substituents. *Trans*-AB-porphyrins are available *via* a number of routes, of which the following were attractive for the structures herein: (1) reaction of a 1,9-bis(*N*,*N*-dimethylaminomethyl)dipyrromethane + a dipyrromethane in the presence of zinc acetate in ethanol followed by oxidation with DDQ,[32] and (2) reaction of a 1,9-bis[(propylimino)-methyl]dipyrromethane + a dipyrromethane in the presence of zinc acetate in ethanol.[33] The latter was utilized to gain access to the desired Step-4 reagents.

The synthesis of **P1-(PO$_4$)$_2$** and **P1-(OH)$_2$** has been reported previously (Chart 1).[38] Porphyrin **P1-(PO$_4$)$_2$** was subjected to enzymatic dephosphorylation in the precipitation experiments (*vide infra*). Porphyrin **P1-(OH)$_2$** was used as an authentic sample for the fully dephosphorylated product. The synthesis of **P1-(PO$_4$)$_2$** employed methyl groups to protect the phosphate moieties during the porphyrin synthesis. The cleavage of the methyl esters in the last step of the synthesis required extensive optimization to avoid cleavage of the phosphate groups.[38] To avoid such complications, we pursued the synthesis of benzyl-protected porphyrin–alkyldiphosphates (Scheme 3).

The synthesis of swallowtail porphyrin–alkyldiphosphate **ZnP2-(PO$_4$Bn)$_2$**, which contains a phenyl moiety rather than a *p*-bromophenyl group, was accomplished using standard procedures.[32,33,38] Commercially available dibenzyl phosphite

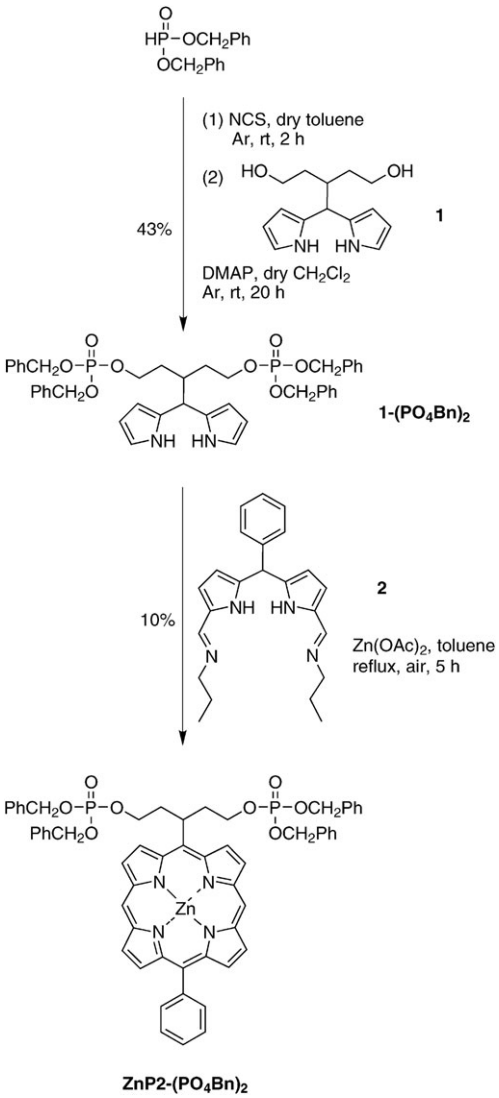

Scheme 3

was treated with *N*-chlorosuccinimide, yielding dibenzyl chlorophosphate.[56] The product was sufficiently pure for use in the subsequent step after removal of the hydroxysuccinimide side-product by filtration. Treatment of dipyrromethane–dicarbinol **1**[38] with the crude dibenzyl chlorophosphate in the presence of a catalytic amount of 4-dimethylaminopyridine (DMAP) yielded dipyrromethane–alkyldiphosphate **1-(PO$_4$Bn)$_2$** in 43% yield. A lesser amount (29%) of the monophosphate derivative was also isolated. The condensation of **1-(PO$_4$Bn)$_2$** and bis[(propylimino)methyl]dipyrromethane **2**[33] in refluxing toluene in the presence of zinc acetate furnished porphyrin–alkyldiphosphate **ZnP2-(PO$_4$Bn)$_2$** in 10% yield (a typical yield for *trans*-AB-porphyrins with these types of substituents). Scaling up the synthesis (1.35 mmol scale) resulted in slightly decreased yields (5–8%).

B. Iodination. The porphyrins to be employed in the enzymatic study, **P1-(PO$_4$)$_2$** and **P2-(PO$_4$)$_2$**, each have two free *meso* positions for the later introduction of ^{131}I. Therefore, we investigated the synthesis of a swallowtail-diphosphate diiodoporphyrin with the following objectives: (1) to

establish the synthetic pathway to such iodoporphyrins, (2) to examine the aqueous solubility of such iodoporphyrins as well as the soluble-to-insoluble conversion, and (3) to potentially employ the cold iodoporphyrin in *in vivo* biodistribution studies. The corresponding hot agent bearing radioiodine may be synthesized in the same manner.

Demetalation of **ZnP2-(PO_4Bn)$_2$** with TFA afforded free-base porphyrin–alkyldiphosphate **P2-(PO_4Bn)$_2$** upon column chromatography in 43% yield. The low yield likely stems from partial cleavage of the benzyl protecting groups.[57] Superior conditions entailed use of *p*-TsOH·H_2O in CH_2Cl_2 for 20 min, which afforded pure **P2-(PO_4Bn)$_2$** by simple aqueous–organic extraction in 96% yield (Scheme 4). Porphyrin **P2-(PO_4Bn)$_2$** is the common precursor of two candidate SPRs, free-base model porphyrin **P2-(PO_4)$_2$** and diiodinated **P2I_2-(PO_4)$_2$**.

Iodination of **P2-(PO_4Bn)$_2$** with a mixture of bis(trifluoroacetoxy)iodobenzene and iodine in $CHCl_3$–pyridine (2 : 1)[58] yielded *meso* diiodoporphyrin **P2I_2-(PO_4Bn)$_2$**. However, the debenzylation of diiodoporphyrin **P2I_2-(PO_4Bn)$_2$** was not successful. Treatment with Pd/C and H_2[59] removed the benzyl protection as well as the iodo groups. Other deprotection conditions, such as TFA[60] and NaI,[61] failed to yield the desired water-soluble iodoporphyrin.

Diiodination of the zinc chelate **ZnP2-(PO_4Bn)$_2$** was significantly faster than that of the corresponding free-base porphyrin, and proceeded in 88% yield under identical conditions. Debenzylation (and demetalation) of **ZnP2I_2-(PO_4Bn)$_2$** was carried out by treatment with TFA containing 5% thiophenol. The diiodo-substituted free-base porphyrin was isolated after neutralization of the reaction mixture with aqueous NaOH, followed by preparative reversed-phase chromatography. The product had poor solubility in water (even upon the addition of base) or in methanol. The Soret band appeared at λ_{max} = 423 nm (MeOH); such a red-shifted spectrum was consistent with the presence of the two iodines attached to the macrocycle, given that unsubstituted *trans*-AB-porphyrins (A = aryl, B = swallowtail) typically absorb near 412 nm.[33,38] Analytical HPLC showed the sample to be pure, however, attempts at more rigorous characterization were hampered by the low solubility of the product, despite the presence of the two phosphates.

An alternative approach was to remove the benzyl groups first and then perform the iodination in aqueous solution. Such aqueous iodination reactions are known.[62] Thus, treatment of **ZnP2-(PO_4Bn)$_2$** with a mixture of thiophenol in TFA (5 : 95) for 2 h at room temperature,[63] followed by neutralization of the sample (aqueous NaOH) and preparative reversed-phase chromatography afforded water-soluble porphyrin **P2-(PO_4)$_2$** in 99% yield as a dark red solid (Scheme 5). It is worth mentioning that this deprotection is significantly milder and

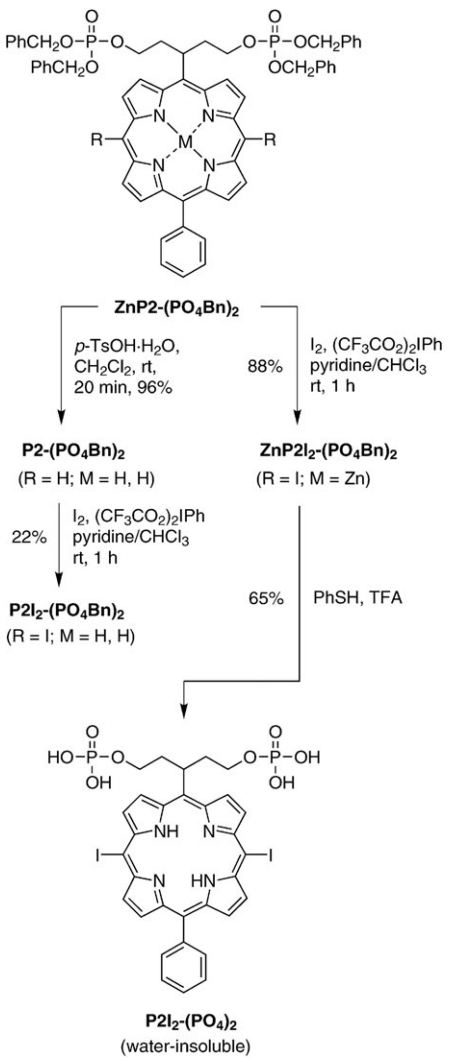

Scheme 4

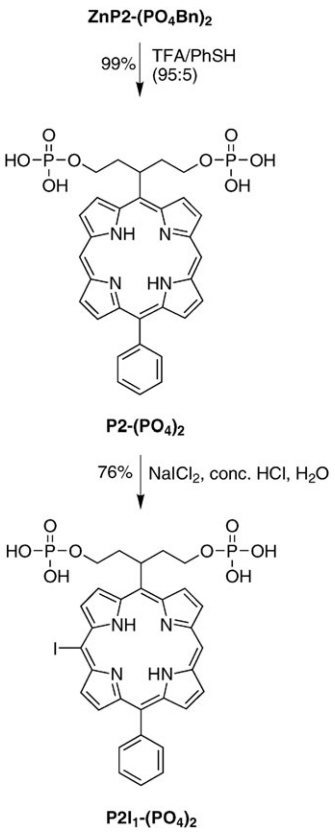

Scheme 5

easier to execute than the method employed previously (TMS–Br, CH_2Cl_2, Ar).[38] None of the dephosphorylated side-products was observed either by ESI-MS or HPLC analysis of the sample.

Iodination of **P2-(PO$_4$)$_2$** in aqueous solution was accomplished with *in situ*-generated $NaICl_2$.[62] Upon addition of the reagent, precipitation occurred, presumably due to the low solubility of the porphyrin–alkyldiphosphate at low pH (conc. HCl solution). Nevertheless the iodination reaction proceeded with high yield (87%), albeit only monosubstitution occurred. Neither uniodinated nor diiodinated products were isolated. The ^{1}H NMR spectrum of pure **P2I$_1$-(PO$_4$)$_2$** clearly showed the disappearance of the broad singlet at 10.32 ppm corresponding to one of the *meso*-proton signals. Thus, the strategy of phosphoester deprotection followed by aqueous-solution iodination proved superior to the route of organic-solution iodination followed by deprotection.

C. Copper insertion. Copper metalation of **P2-(PO$_4$)$_2$** was not possible in water, as the porphyrin–alkyldiphosphates (both protected and unprotected) are sensitive to metal salts in protic solvents.[38] Thus, metalation was carried out at the benzyl phosphate stage in a mixture of $CHCl_3$ and THF (3 : 1) by treatment of **P2-(PO$_4$Bn)$_2$** with $Cu(OAc)_2$ (Scheme 6). The copper chelate **CuP2-(PO$_4$Bn)$_2$** was isolated in 79% yield as a dark orange solid after silica column chromatography. Residual free-base porphyrin was not observed by emission spectroscopic analysis of either the reaction mixture or the pure sample.

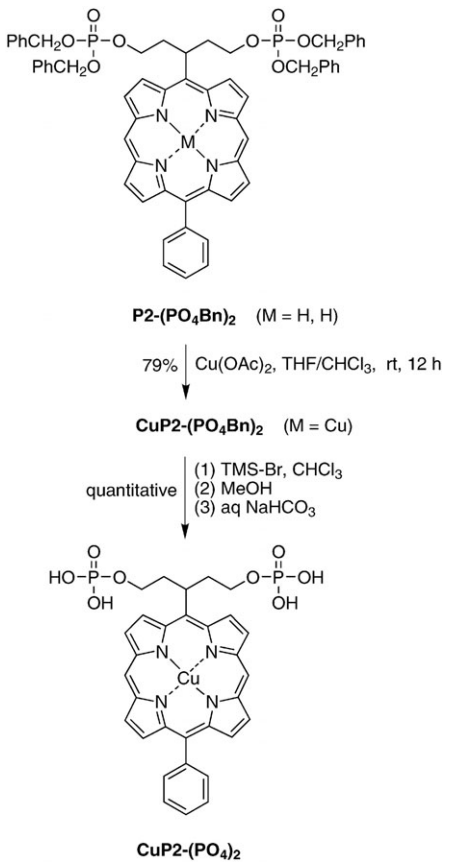

Scheme 6

Attempts to cleave the phosphoester moieties in **CuP2-(PO$_4$Bn)$_2$** were problematic: (i) thiophenol/TFA gave the free-base porphyrin; (ii) TMS–Br in the presence of pyridine[64] gave a complex mixture that contained both partially deprotected and dephosphorylated porphyrins; and (iii) hydrogenation (formic acid, H_2, 10% Pd/C)[65] yielded a mixture of water-soluble copper porphyrins that rapidly decomposed during chromatographic purification. Cleavage of the benzyl protecting groups was eventually accomplished in near-quantitative yield by treatment of **CuP2-(PO$_4$Bn)$_2$** with excess TMS–Br in $CHCl_3$ under an argon atmosphere. The strong acid removed a small fraction of the central copper atoms (as shown by UV-Vis absorption and emission spectroscopy), but the product consisted predominantly of the desired copper porphyrin **CuP2-(PO$_4$)$_2$**.

D. Benchmark compounds. A series of model compounds was prepared as benchmarks for use in the enzymatic reactions. Enzymatic dephosphorylation of **P2-(PO$_4$)$_2$** or **CuP2-(PO$_4$)$_2$** is expected to produce dihydroxyporphyrin **P2-(OH)$_2$** or **CuP2-(OH)$_2$**, respectively. Free-base dihydroxyporphyrin **P2-(OH)$_2$** was synthesized as a reference compound (Scheme 7). Thus, reaction of bis[(propylimino)methyl]dipyrromethane **2** and TBDMS-protected swallowtail dipyrromethane **1-(OTBDMS)$_2$** in the presence of zinc acetate in refluxing toluene gave the porphyrin **ZnP2-(OTBDMS)$_2$** in 32% isolated yield. Cleavage of the TBDMS protecting groups with TBAF followed by demetalation with TFA/CH_2Cl_2 gave **P2-(OH)$_2$** in 93% yield. Treatment of **P2-(OH)$_2$** with $Cu(OAc)_2$ in a mixture of $CHCl_3$ and MeOH (3 : 1) yielded copper chelate **CuP2-(OH)$_2$** in 98% yield after chromatography.

The synthesis of **CuP2-(PO$_4$)$_2$** shown in Scheme 6 relied on copper insertion in organic solution followed by phosphoester deprotection. An alternative synthesis reverses the order of the two steps (Scheme 7). The synthesis of methyl phosphate-substituted porphyrin **CuP2-(PO$_4$Me)$_2$**, of which analogues have been already been reported,[38] was attempted from **CuP2-(OH)$_2$** by treatment with excess dimethyl chlorophosphate in the presence of DMAP. The analogous reaction with zinc or free-base porphyrins results in at most trace amounts of the desired diphosphates, presumably due to zinc-mediated phosphate loss, or interference from the porphyrinic nitrogen atoms, respectively. By contrast, the reaction with **CuP2-(OH)$_2$** proceeded well, and **CuP2-(PO$_4$Me)$_2$** was isolated as a bright orange solid in (unoptimized) 35% yield after silica column chromatography. LD-MS analysis showed the presence of several major peaks in addition to the molecule ion (m/z 768.8), which were assigned to demetalated **P2-(PO$_4$Me)$_2$** (m/z 708.5), and copper or free-base dihydroxyporphyrin **CuP2-(OH)$_2$** (m/z 552.3) or **P2-(OH)$_2$** (m/z 488.4), respectively. We attribute these peaks to demetalation and phosphate cleavage under the analysis conditions, as free-base porphyrin was not observed upon UV-Vis absorption spectroscopic analysis of the sample, and the product was pure by TLC and HPLC analysis.

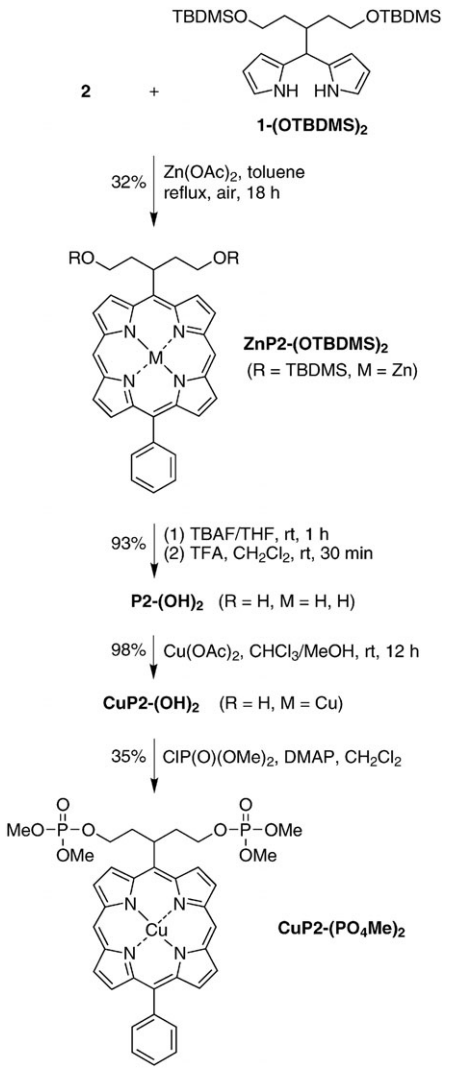

Scheme 7

E. Chemical characterization. All porphyrins were fully characterized by ^{1}H NMR spectroscopy (except copper chelates), LD-MS, high resolution ESI-MS, and UV-Vis absorption and emission spectroscopy. The copper chelates were non-emissive, as expected. LD-MS analysis of each benzyl-protected porphyrin–alkyldiphosphate showed the presence of both the molecule ion and peaks corresponding to the loss or gain of one and two benzylic groups. In two cases [**P2I$_1$-(PO$_4$)$_2$**, **CuP2-(PO$_4$)$_2$**], ESI-MS data were not obtained. The identity of the mono-iodo diphosphate free-base porphyrin **P2I$_1$-(PO$_4$)$_2$** (the non-iodinated precursor of which was fully characterized) was confirmed by ^{1}H NMR spectroscopy (loss of *meso* proton), absorption and emission spectroscopy (red-shifted spectra), and HPLC. The identity of the diphosphate copper porphyrin **CuP2-(PO$_4$)$_2$** (the benzyl-protected precursor of which was fully characterized) was confirmed by water solubilization, absorption spectroscopy, emission spectroscopy, and HPLC.

All but one of the porphyrins bearing free phosphate groups were soluble in pure water. The water-soluble porphyrins include **P1-(PO$_4$)$_2$**, **P2-(PO$_4$)$_2$**, **P2I$_1$-(PO$_4$)$_2$** and **CuP2-(PO$_4$)$_2$**; the water-insoluble porphyrin was **P2I$_2$-(PO$_4$)$_2$**. Each water-soluble porphyrin (as well as the dihydroxyporphyrins) was examined by HPLC. NMR spectra were obtained of the porphyrin–alkyldiphosphates at ~1 mM concentration in D_2O with no noticeable signs of aggregation. At much more dilute concentrations, the absorption spectra of the porphyrin–alkyldiphosphates in water exhibited characteristic absorption bands with no noticeable signs of aggregation. The aqueous solutions of **P2-(PO$_4$)$_2$**, **P2I$_1$-(PO$_4$)$_2$** and **CuP2-(PO$_4$)$_2$** were stable at room temperature for extended periods of time (several days), when shielded from the light.

3 Enzymatic studies

We performed a series of experiments with the water-soluble porphyrins **P1-(PO$_4$)$_2$**, **P2-(PO$_4$)$_2$**, **P2I$_1$-(PO$_4$)$_2$** and **CuP2-(PO$_4$)$_2$** to assess conversion to a precipitate upon enzymatic treatment as required for a porphyrin-based SPR. Extensive experiments were carried out with **P1-(PO$_4$)$_2$**, and representative experiments were then performed with the other three porphyrins.

Porphyrin–alkyldiphosphates were treated in aqueous solution with shrimp alkaline phosphatase (SAP), an enzyme known to rapidly remove phosphate groups. The product of the reaction is expected to be a mono-hydroxyporphyrin or a dihydroxyporphyrin (Scheme 8). Each dihydroxyporphyrin examined herein is expected to be insoluble in water, and hence expected to precipitate. The insolubility of **P1-(OH)$_2$** and **P2-(OH)$_2$** was confirmed by testing with authentic samples. The reaction course was monitored by several methods

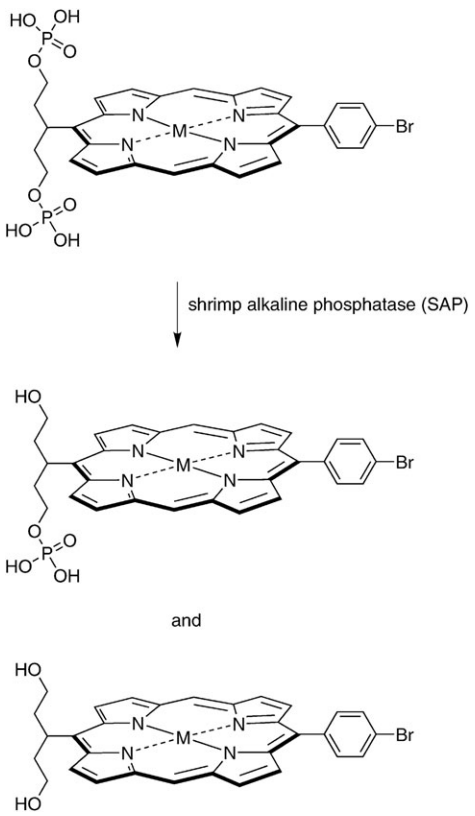

Scheme 8

including visual inspection, absorption spectroscopy, ESI-MS, and nephelometry.

A. Qualitative composition upon enzymatic treatment. The enzymatic treatment was carried out with an aqueous solution of **P1-(PO$_4$)$_2$** at 68 μM in a Tris-HCl buffer (50 mM, pH 9.0) as described in the Experimental section. One enzymatic reaction (E) and three negative control reactions were set up. The controls included use of heat-inactivated enzyme and enzyme buffer (dE), enzyme buffer but no enzyme (MZ), and neither enzyme buffer nor enzyme (NE). All four tubes were incubated at 37 °C for 2 h followed by centrifugation. The results are shown in Fig. 2. Treatment with enzyme afforded rapid discoloration of the reaction mixture (<1 min). After 2 h, no precipitate was observable by visual inspection, but was readily observed upon centrifugation. No significant changes were observed in the absence of enzyme, or with the other two controls (not shown). We note that centrifugation is not essential for eventual visual observation of the precipitate in the case of enzymatic treatment; indeed, a red–brown precipitate was observed at the bottom of the tube after standing for several days.

Absorption spectra and ESI-MS data were obtained for aqueous aliquots removed from the tubes. Any precipitate was isolated, washed with water, dissolved in DMF and analyzed by ESI-MS. The origin of the discoloration of the reaction mixture upon treatment with enzyme is displayed in the absorption spectrum. Prior to the addition of the enzyme SAP, the **P1-(PO$_4$)$_2$** exhibited a strong absorption in aqueous solution at 401 nm (Soret band). Following treatment (prior to or following centrifugation), a sample from the aqueous phase shows extensive broadening (and diminished intensity) of the porphyrin absorption bands. By contrast, the spectrum of the sample without enzyme remains characteristic of a monomeric porphyrin in solution (Fig. 2). The reaction mixtures in tube MZ and dE showed slight decreases (22–25%) in the absorption intensity at 401 nm, which may be attributed to the presence of divalent salts (*e.g.*, Mg^{2+}, Zn^{2+}).

ESI-MS analysis of the supernatant upon enzyme treatment showed peaks corresponding to the dephosphorylated porphyrin **P1-(OH)$_2$** and a small amount of **P1-OH/PO$_4$**. The molecule ions were typically cationized with H^+ and/or Na^+ (see ESI†). It was surprising to observe a peak attributed to **P1-(OH)$_2$**, given that an authentic sample of **P1-(OH)$_2$** does not dissolve appreciably in water, and attempts to obtain an ESI-MS spectrum from an aqueous sample did not give the corresponding peak. Analysis of the precipitate (following isolation and dissolution in DMF) showed that **P1-(OH)$_2$** was the major component. ESI-MS analysis showed the sole presence of starting **P1-(PO$_4$)$_2$** in the control reactions with no enzyme or with enzyme buffer, whereas the mass spectrum of the reaction mixture treated with deactivated enzyme displayed peaks attributed to **P1-(PO$_4$)$_2$**, **P1-(OH)$_2$** and **P1-OH/PO$_4$**. Apparently, the condition that we employed for deactivation (75 °C for 20 min) did not completely deactivate the enzyme. However, the heat treatment did significantly lower the enzyme activity given that **P1-(PO$_4$)$_2$** remained present after incubation for 2 h.

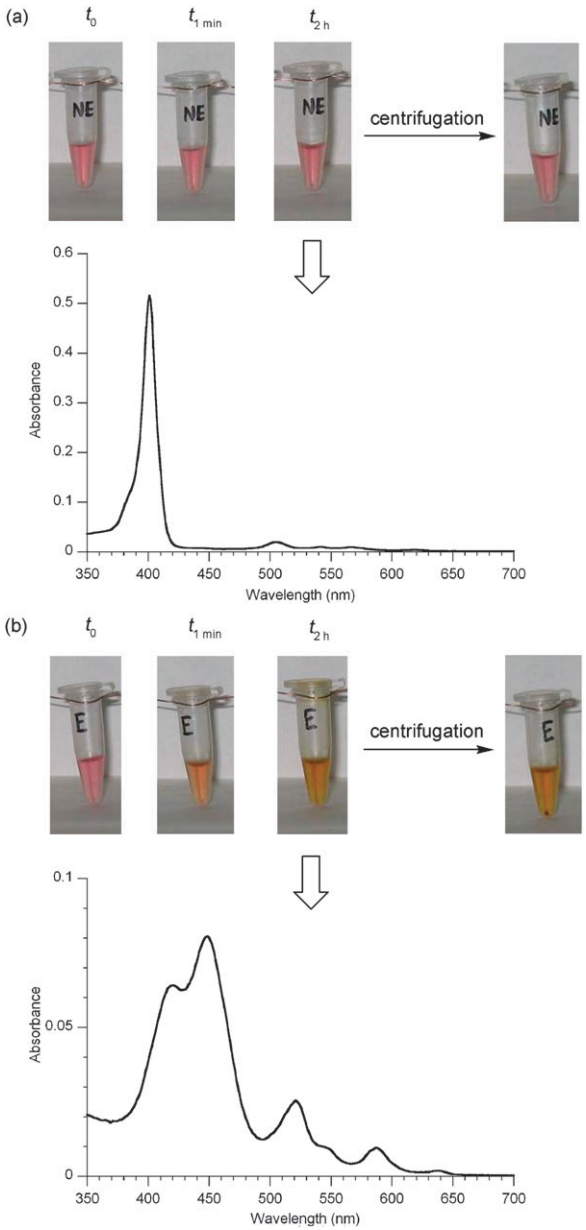

Fig. 2 Time course of **P1-(PO$_4$)$_2$** in aqueous solution with (a) no enzyme (NE) or (b) active SAP (E). Samples with a buffer solution or heat-inactivated SAP gave the same results as with no enzyme (not shown). A brown precipitate is clearly visible following centrifugation of the tube containing enzyme. The absorption spectrum of the aqueous phase following incubation for 2 h shows no aggregation (control reaction lacking enzyme) or extensive aggregation (reaction mixture with enzyme).

B. Kinetic study upon enzymatic treatment. The porphyrin **P1-(PO$_4$)$_2$** at 60 μM in water containing a Tris-HCl buffer (50 mM, pH 9.0) was treated with the enzyme SAP at 37 °C. Aliquots were periodically removed from the reaction tube and heated to deactivate the enzyme (70 °C at 10 min), whereupon absorption spectra were obtained in water at 402 and 450 nm as shown in Fig. 3. The data at 402 nm predominantly measure the concentration of the monomeric intact porphyrin, whereas 450 nm provides a gauge of the amount of aggregated porphyrin (of unknown molar

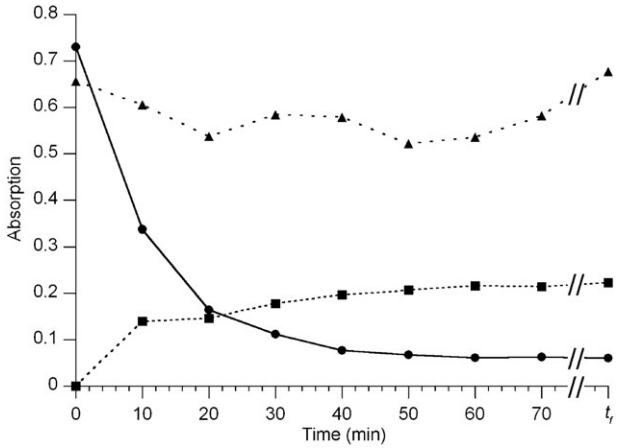

Fig. 3 Absorption spectral monitoring of the reaction course upon treatment of **P1-(PO$_4$)$_2$** with enzyme. Legend: monomeric porphyrin in water (402 nm: solid line, circles); aggregated porphyrin in water (450 nm; dotted line, squares); total porphyrin in DMF (406 nm: dashed line, triangles). The t_f datapoints were collected after overnight reaction.

absorption coefficient). To measure the total porphyrin present, and ensure there was no porphyrin decomposition during the course of the reaction, samples were also removed and dissolved in DMF, which dissolves all of the porphyrin species [substrate porphyrin **P1-(PO$_4$)$_2$** and the hydrolyzed product porphyrins].

The sharp drop in absorption intensity at 402 nm (by more than half in the first 10 min after the addition of enzyme) was accompanied by the intensification of absorption at 450 nm. The peak at 450 nm likely represents aggregated complexes of **P1-(OH)$_2$** and **P1-OH/PO$_4$** [and possible entrainment of some **P1-(PO$_4$)$_2$**]. On the other hand, the absorption intensity at 406 nm determined in DMF changed little during the reaction course. Finally, **P1-(PO$_4$)$_2$** was incubated with enzyme for 5 h, whereupon the entire reaction mixture was dissolved in DMF, thereby eliminating any sampling error caused by taking aliquots from heterogeneous media. The absorption intensity at 406 nm changed little after the incubation (0.61 to 0.65; not shown). Thus, the intensity decrease of the 402 nm peak must stem from aggregation and precipitation of **P1-(OH)$_2$** and/or **P1-OH/PO$_4$** formed *via* enzymatic dephosphorylation.

C. Kinetics of precipitation. We assessed the extent of precipitation during the course of the reaction by nephelometry, a technique that measures scattered light. A nephelometer is readily available by use of a fluorimeter, where the light deflected by the precipitate in the sample in a cuvette is detected at a right angle from the incident beam.[66] For use with porphyrins, the wavelength of the incident beam was chosen as 800 nm to avoid any absorption by the porphyrin.

The dephosphorylation process was carried out with a gently stirred sample of **P1-(PO$_4$)$_2$** at 35 μM in a 3-mL fluorescence cuvette, and the scattered light was measured continuously as a function of time. The porphyrin solution treated with deactivated SAP enzyme gave no increase in the intensity of scattered light over the period examined (2 h). On the other hand, the porphyrin solution treated with active SAP enzyme gave a clear increase in scattered light, steadily increasing above background over the course of ~6 h (Fig. 4A). A slight further increase was observed after 18 to 20 h. Mass analysis showed the presence of **P1-OH/PO$_4$** even when the intensity of the scattered light leveled off. A second batch of SAP was added, but after 6 h the mass peak attributed to **P1-OH/PO$_4$** still remained. The **P1-OH/PO$_4$** mass peak finally disappeared after several days. The slow dephosphorylation may stem from the low temperature (~25 °C instead of 37 °C) inside the nephelometer.

D. Further studies. Water-soluble porphyrin–alkyldiphosphates **P2-(PO$_4$)$_2$**, **P2I$_1$-(PO$_4$)$_2$** and **CuP2-(PO$_4$)$_2$** were treated in the same manner as for **P1-(PO$_4$)$_2$** and monitored by visual inspection, absorption spectroscopy, and nephelometry. The final reaction mixtures were analyzed by HPLC. In each case, the results generally mirrored those described above for **P1-(PO$_4$)$_2$**. Some slight differences were observed by nephelometry, where precipitate formation was more rapid than that observed with **P1-(PO$_4$)$_2$**. In particular, the amount of precipitate increased until approximately 2 h and leveled off thereafter. An example is shown for **P2I$_1$-(PO$_4$)$_2$** (Fig. 4B). When more concentrated porphyrin solutions were employed, precipitate formation could be seen initially, followed by a period of gradual decrease. As a small amount of orange

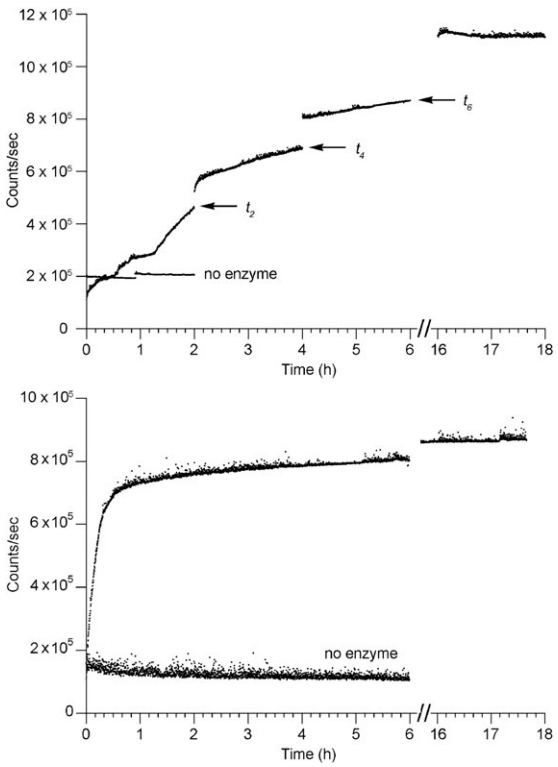

Fig. 4 Light scattering (nephelometry) over time upon treatment of a bis(dihydroxyphosphoryloxy)alkylporphyrin in water with the enzyme SAP. (a) The sample of porphyrin **P1-(PO$_4$)$_2$** was disturbed upon removal of aliquots (for ESI-MS analysis) at 2, 4 and 6 h. (b) The porphyrin **P2I$_1$-(PO$_4$)$_2$**.

coating was observed on the stir bar, the decrease may be due to the formation of large aggregates of porphyrin, which settle out of the suspension. Regardless, in each case, the porphyrins underwent the soluble-to-insoluble conversion upon treatment with the enzyme SAP.

Outlook

A porphyrin-based model compound for use as a Step-4 reagent in the STAR method has been synthesized. The soluble form carries phosphate groups at the termini of a branched alkyl chain. The phosphates can be efficiently cleaved upon treatment with a phosphatase enzyme, resulting in the formation of a precipitate. The potential for radiolabeling has been investigated through iodination and metalation experiments. Each of four porphyrins examined underwent the desired soluble-to-insoluble conversion. Accordingly, it should be possible to employ water-soluble porphyrin–alkylphosphates to deliver radioactive loads to the target, and thereby form an insoluble precipitate as a result of enzymatic action. The syntheses developed herein incorporate iodine or copper (surrogates for radionuclides) near the end of the preparative manipulations, which is highly desirable for medical applications. The ability to form an immobile precipitate *in situ* rather than deliver intact nanoparticles may afford greater control and versatility. It should be noted that while the present porphyrins contain phosphates, other enzymatically cleavable groups such as sulfates or glucuronides also could be employed. In addition, the presence of phosphates may make the radiolabeled analogues of the porphyrins compounds viable alone for some therapies given the overexpression of phosphatases in many cancers.[67]

It warrants emphasis that for the successful development of the STAR method, the design, synthesis, and validation of a Step-4 SPR is a necessary prelude to the design of a Step-1 SPR. Step-1 and Step-4 SPRs have different chemical structures, yet both types of SPRs share the requirement for soluble-to-insoluble conversion, and thus will share some structural features. A Step-1 SPR presents a greater challenge given the requirements to (1) bear a cancer-targeting agent, (2) bear a ligand for binding of the enzyme conjugate (*i.e.*, bispecific or Step-3 reagent), (3) undergo the soluble-to-insoluble conversion, and (4) display the ligand for binding of the enzyme conjugate upon precipitation to give the platform. Molecular designs centered around porphyrins that meet these criteria have been described.[68] The work described herein may provide the basis for refined designs of Step-1 SPRs and ultimately prove useful in new therapeutic approaches for treating solid tumors. By all accounts, the development of radiotherapeutics is in its infancy.[8] Synthetic porphyrins may prove useful for a variety of radiotherapeutic applications given their inherent tailorability and versatility as carriers, either by covalent linkage (*e.g.*, I) or by chelation (*e.g.*, Cu, Ga, Y, Rh, In, Lu, Re, Bi) for essentially all of the radionuclides[8,25,69] that have been identified or proposed in recent years for radiotherapy.

Experimental

General

^{1}H NMR (300 MHz) and ^{13}C NMR (75 MHz) spectra were recorded in $CDCl_3$ unless noted otherwise. Absorption spectra and fluorescence spectra were collected at room temperature in CH_2Cl_2 unless noted otherwise. Hydrophobic porphyrins were analyzed in neat form by laser desorption mass spectrometry (LD-MS).[70] The water-soluble porphyrins were analyzed by direct infusion of water–acetonitrile (40:60) or water–methanol (40 : 60) solutions by atmospheric pressure electrospray mass spectrometry (ESI-MS). Both in LD-MS and ESI-MS analyses, positive ions were detected unless noted otherwise. Benzyl-protected porphyrin–alkyldiphosphates gave clusters of peaks in the molecule ion region that were attributed to the addition or loss of benzyl groups; in each case, the molecule ion only is listed. Solvents were dried according to standard procedures. The solvent $CHCl_3$ contained the inhibitor amylenes or ethanol; the former is distinguished by referral as "$CHCl_3$–amylenes" whereas "$CHCl_3$" refers to the solvent containing ethanol.

Non-commercial compounds

Compounds **1-(OTBDMS)$_2$**,[38] **1**[38] and **2**[33] were synthesized as described in the literature.

Chromatography

Preparative chromatography was performed using silica or alumina (80–200 mesh). Thin layer chromatography was performed on silica or alumina. Transparent samples were visualized by UV-light (254 nm and 365 nm), Br_2-vapor, or $KMnO_4/K_2CO_3$. Reversed-phase preparative column chromatography was carried out using C-18-coated silica and eluants containing water admixed with methanol. Analytical HPLC in all cases was carried out using a reversed-phase C-18 column (5 μm, 4.6 mm × 150 mm) with the following elution program with solvents A (water containing 0.1% TFA) and B (methanol containing 0.1% TFA): flow rate = 1.5 mL min^{-1}; 0–2 min, 0% B; 5–35 min, 0 → 95% B; 35–40 min, 95% B; detection at 254, 400, and 417 nm; void volume typically 1.1 min.

Enzymatic experiments

HPLC-grade water was used to prepare all aqueous solutions and absorption spectral measurements. The concentration of the enzyme SAP in the stock solution was 2.55 μM, calculated from the unit concentration (unit μL^{-1}), specific activity (unit mg^{-1}) and molecular weight (g mol^{-1}; all data provided by Promega). Porphyrin concentrations were calculated from absorption spectra assuming ε_{Soret} = 500 000 M^{-1} cm^{-1}. The enzymatic reaction mixture was analyzed by direct infusion of water–methanol (40 : 60) solutions by ESI-MS in the positive-ion mode.

(i) Reaction composition. The free-base porphyrin **P1-(PO$_4$)$_2$** shows good solubility in water; however, the porphyrin needs to be soluble in a buffer suitable for the dephosphorylation reaction catalyzed by SAP. Mixing the aqueous solution of the porphyrin and a buffer solution from the enzyme

provider (Promega) yielded an immediate red precipitate. Aqueous solutions of **P1-$(PO_4)_2$** of a range of concentrations (up to 0.61 mM) were prepared and mixed with the SAP buffer. With high concentrations of porphyrin, a precipitate was observed (by visual inspection) to form very rapidly. With low concentrations, a precipitate was observed only upon centrifugation of the sample. In each case, the porphyrin concentration in the supernatant (calculated from absorption spectra) was 1–2 μM. To avoid such precipitation, a Tris-HCl buffer (50 mM, pH 9.0) was used (lacking SAP and metal salt) to prepare the porphyrin solution. Neither precipitation nor change of color in the solution was observed. Although the lack of Mg^{2+}, which is a cofactor of SAP, may lower the enzyme activity, a higher starting substrate concentration is preferable to better distinguish the reaction composition before and after dephosphorylation. On the other hand, the lower enzyme activity can be compensated for by increasing the enzyme/substrate ratio. After several preliminary experiments, we found that a suitable molar ratio of phosphoester [each **P1-$(PO_4)_2$** molecule contains two phosphoesters] to SAP is approximately 5000 : 1.

(ii) Representative protocol for qualitative analysis. A solution of **P1-$(PO_4)_2$** in 1600 μL of a Tris-HCl buffer (50 mM, pH 9.0) was prepared. A 60-μL aliquot of this solution was diluted in 3 mL of water, and an absorption spectrum was obtained. The concentration calculated from the intensity at 401 nm was 68 μM. The remaining porphyrin solution was distributed evenly into four 1.5-mL Eppendorf tubes, of which one received the enzyme and enzyme buffer (tube E), and three were used for controls (enzyme buffer and heat-deactivated enzyme, dE; enzyme buffer but no enzyme, MZ; and neither enzyme buffer nor enzyme, NE). A 3.8-μL aliquot of the SAP stock solution [containing 1 mM $MgCl_2$, 0.1 mM $ZnCl_2$, 25 mM Tris-HCl (pH 7.6) and 50% (v/v) glycerol] was added to tube E. Another 3.8 μL of the SAP stock solution was heated at 75 °C for 20 min and then added to tube dE. A buffer solution was prepared, which contained 1 mM $MgCl_2$, 0.1 mM $ZnCl_2$, 20 mM Tris-HCl (pH 7.2) and 40% (v/v) glycerol. A 3.8-μL aliquot of the buffer solution was added to tube MZ. All four tubes were incubated at 37 °C for 2 h and then centrifuged at 7,000 rpm for 8 min. From each tube, 60 μL of the solution (tube dE, NE and MZ) or supernatant (tube E) was transferred into 3 mL of water for absorption analysis. The remaining solutions and supernatant were used for mass analysis. The precipitate in tube E was washed with water, dissolved in DMF, and analyzed by ESI-MS.

(iii) Protocol for kinetics experiments. A solution of **P1-$(PO_4)_2$** in 500 μL of a Tris-HCl buffer (50 mM, pH 9.0) was prepared in an Eppendorf tube at a concentration of 60 μM. A 5.3-μL aliquot of the SAP stock solution was added, and the tube was incubated at 37 °C with shaking. A 50-μL aliquot of the reaction mixture was removed from tube 1 every 10 min from 0 min (before the addition of SAP) to 70 min. The remaining solution was incubated at 37 °C for 16 h, and then heated to 70 °C for 10 min. Each aliquot was heated to 70 °C in a water bath for 10 min to deactivate the enzyme. Absorption spectra in both water and DMF were recorded for each aliquot and the remaining solution.

A solution of **P1-$(PO_4)_2$** in 300 μL of a Tris-HCl buffer (50 mM, pH 9.0) was prepared in an Eppendorf tube at a concentration of 38 μM. A 100-μL aliquot of the solution was transferred to a cuvette filled with 3 mL of DMF, and the absorption spectrum was recorded. A 1.7-μL aliquot of the SAP stock solution was added to the Eppendorf tube, and the reaction was incubated at 37 °C with shaking for 5 h. The entire reaction mixture was transferred to a cuvette filled with 3 mL of DMF, and a second absorption spectrum was recorded. The absorption intensity at 406 nm in the second spectrum was divided by 2 and compared to the absorption intensity at 406 nm in the first spectrum.

(iv) Protocol for precipitate detection. A simple light-scattering instrument (nephelometer)[66] was constructed using a fluorimeter (Photon Technology International). Excitation and emission monochromators were both set at the same wavelength to allow scattered incident light to enter the photomultiplier. The wavelength 800 nm was chosen to minimize direct absorption by the porphyrin. The instrument parameters were as follows: photomultiplier voltage, 800 V; slit widths, 1 mm; integration time, 10 s. The enzymatic reaction was performed in a 1-cm pathlength fluorescence cuvette (3 mL) at room temperature. The cuvette was equipped with a stirring bar, and the reaction mixture was stirred at a modest rate (no vortex formation). The data are obtained as counts/sec over time.

A fluorescence cuvette was filled with 3 mL of an aqueous solution of **P1-$(PO_4)_2$** in a Tris-HCl buffer (50 mM, pH 9.0). The concentration of the porphyrin solution was 35 μM. An aliquot (16.8 μL) of the SAP stock solution was added to the cuvette, and the light scattering measurement was started immediately. A 500-μL aliquot of the reaction mixture was taken out of the cuvette for mass analysis at 2, 4, 6 and 18 h. After the mass spectrum was obtained, the aliquot was transferred back to the cuvette to keep the total volume constant. A second batch of SAP (16.8 μL) was added at 20 h, and the cuvette was stirred at room temperature. ESI-MS spectra were obtained every 2 h by the same procedure described above.

For **P2-$(PO_4)_2$** and **CuP2-$(PO_4)_2$**, the reactions were monitored over 3 h by nephelometry. At the end of the reaction, an aliquot of each sample was diluted with methanol, and the sample was analyzed by HPLC with **P2-$(OH)_2$** or **CuP2-$(OH)_2$** as reference. For **P2I$_1$-$(PO_4)_2$**, the reaction was monitored over 18 h by nephelometry.

5-[1,5-Bis(dibenzyloxyphosphoryloxy)pent-3-yl]dipyrromethane (1-$(PO_4Bn)_2$)

Following a literature procedure,[56] a solution of *N*-chlorosuccinimide (612 mg, 4.57 mmol) in dry toluene (25 mL) was treated with dibenzyl phosphite (1.01 mL, 4.57 mmol) under argon at room temperature for 2 h. The reaction mixture was filtered through a filter paper. The filtrate was concentrated and dried under vacuum. The resulting colorless liquid was dissolved in dry CH_2Cl_2 (10 mL) to afford the "dibenzyl chlorophosphate solution." Following a literature procedure[38] with modifications, the dibenzyl chlorophosphate solution was

slowly added to a solution of **1** (260 mg, 0.935 mmol) and DMAP (557 mg, 4.57 mmol) in dry CH_2Cl_2 (10 mL). The mixture was stirred under argon at room temperature for 20 h. The reaction mixture was diluted in CH_2Cl_2 and washed with water. The organic layer was dried (Na_2SO_4). Removal of solvent gave the crude product as a dark oil. Chromatography [silica, CH_2Cl_2–MeOH (49 : 1)] of the crude product yielded a light-yellow, viscous oil (309 mg, 43%): ^{1}H NMR δ 1.40–1.50 (m, 2H), 1.69–1.79 (m, 2H), 2.20–2.30 (m, 1H), 3.87–3.94 (m, 4H), 4.19 (d, J = 4.8 Hz, 1H), 4.94–5.04 (m, 8H), 5.91–5.95 (m, 2H), 6.07–6.11 (m, 2H), 6.60–6.64 (m, 2H), 7.29–7.36 (m, 20H), 8.57 (br, 2H); ^{13}C NMR δ 32.26, 32.32, 35.35, 40.59, 66.27, 66.33, 69.46, 69.51, 106.72, 108.21, 117.04, 128.09, 128.13, 128.73, 128.76, 130.83, 135.86, 135.92; FAB-MS obs. 769.2841, calc. 769.2808 [(M + H)$^+$, M = $C_{42}H_{46}N_2O_8P_2$]. Anal. Calc. for $C_{42}H_{46}N_2O_8P_2$: C, 65.62; H, 6.03; N, 3.64. Found: C, 65.67; H, 6.03; N, 3.61%.

Data for 5-[1-(dibenzyloxyphosphoryloxy)-5-hydroxypent-3-yl]dipyrromethane (1-OH/PO_4Bn)

5-[1-(Dibenzyloxyphosphoryloxy)-5-hydroxypent-3-yl]dipyrromethane, which is more polar than 5-[1,5-bis(dibenzyloxyphosphoryloxy)pent-3-yl]dipyrromethane by TLC analysis, was also isolated as a light-purple, viscous oil (207 mg, 29%): ^{1}H NMR δ 1.34–1.44 (m, 1H), 1.46–1.56 (m, 1H), 1.61–1.70 (m, 1H), 1.72–1.81 (m, 2H), 2.32–2.41 (m, 1H), 3.51–3.60 (m, 2H), 3.86–4.02 (m, 2H), 4.17 (d, J = 5.7 Hz, 1H), 4.95–5.05 (m, 4H), 5.95–6.00 (m, 2H), 6.08–6.12 (m, 2H), 6.59–6.62 (m, 2H), 7.29–7.38 (m, 10H), 8.66 (br, 1H), 8.69 (br, 1H); ^{13}C NMR δ 29.76, 32.84, 32.89, 34.71, 35.23, 41.23, 60.85, 66.66, 66.72, 69.58, 69.64, 106.61, 106.85, 108.14, 108.21, 116.96, 117.03, 128.14, 128.16, 128.81, 131.34, 131.62, 135.80, 135.87; FAB-MS: obs. 508.2143, calc. 508.2127 ($C_{28}H_{33}N_2O_5P$).

Zn(II)-5-[1,5-Bis(dibenzyloxyphosphoryloxy)pent-3-yl]-15-phenylporphyrin (ZnP2-(PO_4Bn)$_2$)

Following a literature procedure,[33,38] a solution of **1-(PO_4Bn)$_2$** (175 mg, 228 μmol) and **2** (103 mg, 286 μmol) in toluene (25 mL) was treated with $Zn(OAc)_2$ (417 mg, 2.28 mmol). The mixture was refluxed open to air for 4.5 h. The reaction mixture was cooled to room temperature and diluted in CH_2Cl_2. The resulting dark solution was washed with water and brine. The organic layer was separated, dried (Na_2SO_4) and concentrated to dryness. Chromatography [silica, CH_2Cl_2–ethyl acetate (4 : 1)] yielded a red solid. The resulting crude product was chromatographed [silica, hexanes–ethyl acetate (2 : 3)] to yield a red solid (25 mg, 10%): ^{1}H NMR δ 2.36–2.48 (m, 2H), 2.78–2.95 (m, 6H), 3.32–3.43 (m, 2H), 3.48–3.72 (m, 6H), 5.13–5.23 (m, 1H), 6.30 (d, J = 7.4 Hz, 2H), 6.37 (d, J = 7.7 Hz, 2H), 6.70–6.82 (m, 8H), 6.85–6.91 (m, 4H), 7.69–7.80 (m, 3H), 8.13 (d, J = 6.6 Hz, 2H), 9.02–9.08 (m, 3H), 9.29 (d, J = 4.4 Hz, 1H), 9.33 (d, J = 4.7 Hz, 1H), 9.36 (d, J = 4.4 Hz, 1H), 9.45 (d, J = 4.7 Hz, 1H), 9.52 (d, J = 4.4 Hz, 1H), 10.01 (s, 1H), 10.20 (s, 1H); LD-MS: obs. 1071.0; FAB-MS: obs. 1070.2572, calc. 1070.2552 ($C_{59}H_{52}N_4O_8P_2Zn$); λ_{abs} 408, 538, 635 nm.

5-[1,5-Bis(dibenzyloxyphosphoryloxy)pent-3-yl]-15-phenylporphyrin (P2-(PO_4Bn)$_2$). Method A

Following a literature procedure,[38] a solution of **ZnP2-(PO_4Bn)$_2$** (25 mg, 23 μmol) in CH_2Cl_2 (4 mL) was treated with TFA (500 μL) at room temperature under argon for 2 h. The reaction mixture was concentrated to dryness and dissolved in CH_2Cl_2. The resulting solution was diluted in CH_2Cl_2 and washed with saturated aqueous $NaHCO_3$. The organic layer was separated and dried (Na_2SO_4). Removal of the solvent yielded the crude product as a dark solid, which upon chromatography (silica, ethyl acetate) gave a purple solid (10 mg, 43%): ^{1}H NMR δ −2.92 (br, 1H), −2.86 (br, 1H), 2.97–3.07 (m, 2H), 3.28–3.39 (m, 2H), 3.76–3.84 (m, 2H), 3.93–4.01 (m, 2H), 4.39–4.50 (m, 6H), 4.58–4.65 (m, 2H), 5.59–5.69 (m, 1H), 6.71–6.76 (m, 2H), 6.78–6.82 (m, 2H), 6.83–6.94 (m, 8H), 6.94–7.00 (m, 4H), 7.79–7.84 (m, 3H), 8.24–8.29 (m, 2H), 9.05–9.09 (m, 2H), 9.30 (d, J = 4.7 Hz, 1H), 9.34 (d, J = 4.7 Hz, 1H), 9.39 (d, J = 4.4 Hz, 1H), 9.42 (d, J = 4.7 Hz, 1H), 9.56 (d, J = 4.7 Hz, 1H), 9.67 (d, J = 4.7 Hz, 1H), 10.19 (s, 1H), 10.27 (s, 1H); LD-MS: obs. 1009.5; ESI-MS: obs. 1009.3491, calc. 1009.3489 [(M + H)$^+$, M = $C_{59}H_{54}N_4O_8P_2$]; λ_{abs} 406, 503, 536, 576, 631 nm.

5-[1,5-Bis(dibenzyloxyphosphoryloxy)pent-3-yl]-15-phenylporphyrin (P2-(PO_4Bn)$_2$). Method B

A solution of **ZnP2-(PO_4Bn)$_2$** (50.2 mg, 0.0469 mmol) in CH_2Cl_2 (14.5 mL) was treated with p-TsOH·H_2O (522 mg, 2.73 mmol) at room temperature for 20 min. The solution was diluted in CH_2Cl_2 and washed with saturated aqueous $NaHCO_3$ solution. The organic layer was dried (Na_2SO_4). Removal of the solvent yielded the crude product as a dark solid that was sufficiently pure (>95%) without further purification (45.4 mg, 96%). Characterization data (^{1}H NMR, LD-MS, λ_{abs}) were identical to those reported with Method A. λ_{em} (λ_{exc} 408 nm) 634, 700 nm.

5-[1,5-Bis(dibenzyloxyphosphoryloxy)pent-3-yl]-10,20-diiodo-15-phenylporphyrin (P2I_2-(PO_4Bn)$_2$)

Following a literature procedure[58] with modification, a solution of bis(trifluoroacetoxy)iodobenzene (57 mg, 134 μmol) and iodine (34 mg, 134 μmol) in $CHCl_3$–amylenes (1 mL) was treated with anhydrous pyridine (500 μL) at room temperature for 30 min. The color of the reaction mixture changed from purple to light yellow. A white solid was observed in the reaction mixture. The resulting yellowish mixture was slowly added to a solution of **P2-(PO_4Bn)$_2$** (9.0 mg, 8.9 μmol) in $CHCl_3$–amylenes (1 mL). The mixture was stirred at room temperature for 1 h. The reaction mixture was diluted in CH_2Cl_2 and washed with saturated aqueous $Na_2S_2O_3$. The organic layer was separated and dried (Na_2SO_4). Removal of the solvent yielded the crude product as a dark purple solid. Chromatography [silica, CH_2Cl_2–ethyl acetate (1 : 1)] yielded a purple solid (2.5 mg, 22%): ^{1}H NMR δ −2.71, 2.89–3.03 (m, 2H), 3.15–3.28 (m, 2H), 3.72–3.84 (m, 2H), 3.92–4.04 (m, 2H), 4.41–4.57 (m, 6H), 4.60–4.70 (m, 2H), 5.46–5.58 (m, 1H), 6.75–6.81 (m, 4H), 6.85–7.03 (m, 16H), 7.72–7.84 (m, 3H), 8.12 (d, J = 7.4 Hz, 1H), 8.70–8.79 (m, 2H), 9.36 (d, J = 4.4 Hz, 1H), 9.51 (d, J = 4.7 Hz, 1H), 9.56 (d, J = 4.7 Hz, 1H),

9.60 (d, J = 4.4 Hz, 2H), 9.72 (d, J = 5.0 Hz, 1H); LD-MS: obs.; FAB-MS: obs. 1261.1421, calc. 1261.1422 [(M + H)$^+$, M = $C_{59}H_{52}I_2N_4O_8P_2$]; λ_{abs} 426, 524, 563, 604, 664 nm.

Zn(II)-5-[1,5-Bis(*tert*-butyldimethylsilyloxy)pent-3-yl]-15-phenylporphyrin (ZnP2-(OTBDMS)$_2$)

Following a standard procedure,[33] a solution of **2** (258 mg, 0.716 mmol) and **1-(OTBDMS)$_2$** (341 mg, 0.716 mmol) in toluene (78 mL) was treated with $Zn(OAc)_2$ (1.35 g, 7.16 mmol). The mixture was refluxed for 18 h open to the air. The toluene was evaporated, and the resulting residue was chromatographed (silica, CH_2Cl_2) to give a purple solid (176 mg, 32%): ^{1}H NMR δ −0.14 (s, 12H), 0.89 (s, 18H), 3.07–3.14 (m, 2H), 3.32-3.39 (m, 2H), 3.61–3.72 (m, 4H), 5.98 (m, 1H), 7.80 (app s, 3H), 8.18–8.20 (m, 2H), 9.05 (s, 2H), 9.31–9.34 (m, 2H), 9.47–9.50 (m, 2H), 9.92–9.93 (m, 1H), 10.08–10.09 (m, 1H), 10.18 (s, 1H), 10.22 (s, 1H); LD-MS: obs. 778.9; ESI-MS: obs. 779.31444, calc. 779.31495 [(M + H)$^+$, M = $C_{43}H_{54}N_4O_2Si_2Zn$]; λ_{abs} 407, 538 nm; λ_{em} (λ_{exc} 407 nm) 578, 631 nm.

5-(1,5-Dihydroxypent-3-yl)-15-phenylporphyrin (P2-(OH)$_2$)

A solution of **ZnP2-(TBDMS)$_2$** (140 mg, 0.179 mmol) was dissolved in THF containing TBAF (3.6 mL of 1.0 M solution, water content ~5%). The reaction was allowed to proceed for 1 h. The sample was concentrated. The residue was dissolved in CH_2Cl_2 (2 mL). The solution was treated with TFA (2 mL). The mixture was stirred at room temperature for 30 min. The mixture was concentrated at reduced pressure. The residue was dissolved in ethyl acetate, and the resulting solution was washed with water. The aqueous layer was extracted with ethyl acetate. The combined organic extract was washed with water, dried (Na_2SO_4), and concentrated. Column chromatography [neutral alumina, CH_2Cl_2–MeOH (98 : 2 → 90 : 10] afforded a bright purple solid (85 mg, 97%): ^{1}H NMR ($CDCl_3$–CD_3OD) δ 3.03–3.08 (m, 2H), 3.25–3.31 (m, 2H), 3.58–3.60 (m, 4H), 5.73 (m, 1H), 7.78 (app s, 3H), 8.21 (app s, 2H), 9.03–9.04 (m, 2H), 9.37–9.40 (m, 2H), 9.46–9.48 (m, 2H), 9.76–9.78 (m, 2H), 9.88–9.89 (m, 1H), 10.29–10.30 (s, 1H); LD-MS: obs. 489.2; FAB-MS: obs. 488.2207, calc. 488.2212 ($C_{31}H_{28}N_4O_2$); λ_{abs} 404, 502, 534, 576 nm; λ_{em} (λ_{exc} 404 nm) 634, 701 nm; HPLC t_R = 32.20 min.

Cu(II)-5-(1,5-Dihydroxypent-3-yl)-15-phenylporphyrin (CuP2-(OH)$_2$)

A sample of **P2-(OH)$_2$** (11.9 mg, 0.0246 mmol) in $CHCl_3$–MeOH (3 : 1, 2 mL) was treated with $Cu(OAc)_2$ (44.5 mg, 0.246 mmol, 10 equiv). Stirring was continued for 12 h at room temperature. The sample was diluted with ethyl acetate and water. The layers were separated, and the aqueous layer was extracted with ethyl acetate. The organic layer was dried (Na_2SO_4). Chromatography [neutral alumina, CH_2Cl_2–MeOH–THF (100 : 0 : 0 → 5 : 1 : 1)] yielded an orange solid (13.2 mg, 98%): LD-MS: obs. 487.4 (M − Cu)$^+$, 548.8 (M$^+$); FAB-MS: obs. 489.2277, calc. 489.2285 [(M − Cu)$^+$ M = $C_{31}H_{28}CuN_4O_2$]; λ_{abs} 403, 530 nm; HPLC t_R = 30.53 (**P2-(OH)$_2$**), 35.76 (**CuP2-(OH)$_2$**), 32.56 (minor), 36.75 (minor) min.

5-[1,5-Bis(dihydroxyphosphoryloxy)pent-3-yl]-15-phenylporphyrin (P2-(PO4)$_2$)

A solution of **1** (22.7 mg, 22.5 mmol) in TFA (4.25 mL) was treated with thiophenol (0.25 mL) at room temperature for 2 h. The solution was neutralized with concentrated aqueous NaOH, and applied onto a reversed-phase silica column equilibrated with H_2O. Elution with H_2O–MeOH (0 → 50%) yielded a dark purple solution that was concentrated *in vacuo*. The resulting dark purple residue was dissolved in distilled water, and the resulting solution was filtered through a plug of cotton wool. The filtrate was freeze-dried to yield a dark red film (quantitative): ^{1}H NMR δ 3.53–3.60 (m, 4H), 3.91 (m, 2H), 4.30 (m, 2H), 5.85 (m, 1H), 7.58 (d, J = 6.0 Hz, 2H), 7.73–7.76 (m, 2H), 7.87–7.91 (m, 1H), 8.39 (br 1H), 8.49 (br 1H), 8.86 (br 1H), 9.05 (br 1H), 9.65 (br, 1H), 9.76 (br 1H), 9.96 (br 1H), 10.16 (br 1H), 10.42 (br, 1H), 10.32 (br, 1H); ESI-MS: obs. 649.1629; calc. 649.1611 [(M + H)$^+$; M = $C_{31}H_{30}N_4O_8P_2$]; λ_{abs} (H_2O) 401, 505, 540, 568, 619; λ_{em} (λ_{exc} 401 nm) 627, 690 nm; HPLC t_R = 16.62 min.

5-[1,5-Bis(dihydroxyphosphoryloxy)pent-3-yl]-10-iodo-15-phenylporphyrin (P2I$_1$-(PO$_4$)$_2$)

Following a literature procedure[62] with modification, a solution of $NaICl_2$ [prepared from aqueous NaOCl (10–13%, 49 μL), NaI (22 mg, 147 mmol) and conc. HCl (28 μL)] was added to a solution of **P2-(PO$_4$Bn)$_2$** (15 mg, 0.023 mmol) in water (600 μL). A solid precipitate formed immediately. The mixture was stirred at room temperature for 12 h. The reaction mixture was diluted by dropwise addition of aqueous NaOH (2.5 M) until all solid dissolved. The resulting solution was applied onto a reversed-phase silica column equilibrated with water. Chromatography [H_2O–MeOH (0 → 50%)] yielded a purple solution. The sample was concentrated *in vacuo*, and the resulting solid residue was dissolved in water. The solution was filtered through a plug of cotton wool. The filtrate was freeze-dried to yield a dark red, voluminous solid (15.4 mg, 87%): ^{1}H NMR δ 3.93 (m, 2H), 4.30 (m, 2H), 5.81 (m, 1H), 7.31–7.62 (m, 5H), 8.10 (m, 1H), 8.22 (m, 1H), 8.48 (m, 1H), 8.71 (m, 1H), 9.47 (br, 1H), 9.9.65 (br, 1H), 9.91 (br, 1H), 10.15 (br, 1H), 10.26 (br, 1H); λ_{abs} (H_2O) 412, 563 nm; λ_{em} (H_2O, λ_{exc} 412 nm) 621, 677 nm; HPLC t_R = 26.02 min.

Cu(II)-5-[1,5-Bis(dibenzyloxyphosphoryloxy)pent-3-yl]-15-phenylporphyrin (CuP2-(PO$_4$Bn)$_2$)

A solution of **P2-(PO$_4$Bn)$_2$** (23.9 mg, 0.0237 mmol) in $CHCl_3$–THF (3 mL, 2 : 1) was treated with $Cu(OAc)_2$ (42.9 mg, 0.237 mmol, 10 equiv). The mixture was stirred at room temperature for 12 h. The reaction mixture was diluted with CH_2Cl_2 and water. The phases were separated, and the aqueous layer was extracted with CH_2Cl_2. The organic layer was dried (Na_2SO_4) and concentrated. Chromatography [silica, CH_2Cl_2–ethyl acetate (4 : 1)] yielded an orange solid (20.0 mg, 79%): LD-MS: obs. 1069.7; ESI-MS: obs. 1070.26165, calc. 1070.26252 [(M + H)$^+$, M = $C_{59}H_{52}CuN_4O_8P_2$]; λ_{abs} 404, 529 nm.

Cu(II)-5-[1,5-Bis(dimethoxyphosphoryloxy)pent-3-yl]-15-phenylporphyrin (CuP2-$(PO_4Me)_2$)

A solution of **P2-$(OH)_2$** (9.80 mg, 0.0182 mmol) in dry CH_2Cl_2 (500 μL) under argon was treated with DMAP (44.4 mg, 0.364 mmol, 10 equiv). The mixture was stirred at room temperature for 10 min, after which dimethyl chlorophosphate (40 μL, 0.37 mmol) was added dropwise. The mixture was stirred at room temperature for 12 h. The mixture was loaded onto a silica column. Chromatography [CH_2Cl_2–MeOH (0 → 3%)] yielded a bright orange solid (5.4 mg, 35%): LD-MS: obs. 768.8 (**CuP2-$(PO_4Me)_2$**$^+$), 708.5 [**P2-$(PO_4Me)_2$**$^+$], 552.3 [**CuP2-$(OH)_2$**$^+$], 525.2 (unassigned), 497.0 (unassigned), 488.4 [**P2-$(OH)_2$**$^+$]; FAB-MS: obs. 765.1310, calc. 765.1304 ($C_{35}H_{36}CuN_4O_8P_2$); λ_{abs} 404, 529 nm.

Cu(II)-5-[1,5-Bis(dihydroxyphosphoryloxy)pent-3-yl]-15-phenylporphyrin (CuP2-$(PO_4)_2$)

A solution of **CuP2-$(PO_4Bn)_2$** (9.6 mg, 0.0090 mmol) in $CHCl_3$–amylenes (500 μL) was treated with TMS-Br (30 μL) at room temperature for 30 min. MeOH (1 mL) was added, and stirring was continued for 20 min. The sample was concentrated. The solid residue was dissolved in dilute aqueous $NaHCO_3$, and the resulting solution was applied onto a reversed-phase silica column equilibrated with H_2O. Elution with H_2O–MeOH (0 → 50%) yielded a dark orange solution that was concentrated *in vacuo*. The resulting dark orange residue was dissolved in distilled water, and the resulting solution was filtered through a plug of cotton wool. The filtrate was freeze-dried to yield a dark red voluminous solid (quantitative): λ_{abs} (H_2O) 400, 530; HPLC t_R = 26.56 min.

Zn(II)-5-[1,5-Bis(dibenzyloxyphosphoryloxy)pent-3-yl]-15-phenyl-10,20-diiodoporphyrin (ZnP2I_2-$(PO_4Bn)_2$)

Following a literature procedure[58] with modification, a solution of bis(trifluoroacetoxy)iodobenzene (57 mg, 130 μmol) and iodine (34 mg, 130 μmol) in $CHCl_3$–amylenes (1 mL) was treated with anhydrous pyridine (500 μL) at room temperature for 30 min. The color of the reaction mixture changed from purple to light yellow. The resulting yellow solution was slowly added to a solution of **ZnP2-$(PO_4Bn)_2$** (40 mg, 37 μmol) in $CHCl_3$–amylenes (1 mL). The mixture was stirred at room temperature for 1 h. The reaction mixture was diluted in CH_2Cl_2, and washed with saturated aqueous $Na_2S_2O_3$. The organic layer was separated and dried (Na_2SO_4). Removal of the solvent yielded the crude product as a dark purple solid. Chromatography [silica, CH_2Cl_2/ethyl acetate (0 → 50%)] yielded a dark green solid (44 mg, 88%): ^{1}H NMR δ 2.89–3.03 (m, 2H), 3.12–3.27 (m, 2H), 3.72–3.81 (m, 2H), 3.88–3.99 (m, 2H), 4.47–4.66 (m, 6H), 4.72–4.78 (m, 2H), 5.55–5.61 (m, 1H), 6.39–6.47 (m, 8H), 6.88–6.99 (m, 12H), 7.65–7.75 (m, 3H), 8.01 (d, J = 7.2 Hz, 2H), 8.75–8.76 (m, 2H), 9.09 (d, J = 3.9 Hz, 1H), 9.29 (d, J = 4.8 Hz, 1H), 9.43 (d, J = 4.2 Hz, 1H), 9.59 (d, J = 4.8 Hz, 1H), 9.66 (d, J = 4.5 Hz, 1H), 9.82 (d, J = 4.8 Hz, 1H); LD-MS: obs. 1326.0; FAB-MS: obs. 1324.11, calc. 1323.06 [(M + H)$^+$, M = $C_{59}H_{50}I_2N_4O_8P_2Zn$]; λ_{abs} 434, 567, 617 nm.

5-[1,5-Bis(dihydroxyphosphoryloxy)pent-3-yl]-15-phenyl-10,20-diiodoporphyrin (P2I_2-$(PO_4)_2$)

A solution of **ZnP2I_2-$(PO_4Bn)_2$** (30.4 mg, 0.0230 mmol) in TFA (1.90 mL) was treated with thiophenol (0.10 mL) at room temperature for 2 h. The solution was neutralized with concentrated aqueous NaOH, and applied onto a reversed-phase silica column equilibrated with H_2O. Elution with H_2O–MeOH (0 → 50%) yielded a dark green solution that was concentrated *in vacuo*. The dark purple residue was dissolved in distilled water. The resulting solution was filtered through a plug of cotton wool. The filtrate was freeze-dried to yield a dark green film that proved too insoluble in either aqueous or organic solvents for sufficient characterization (13.4 mg, 65%): λ_{abs} (MeOH) 423, 525, 564, nm; t_R = 34.59 min, t_{col} = 1.09 min.

Acknowledgements

This work was supported by the NIH (GM36238) and by Oncologic, Inc. Mass spectra were obtained at the Mass Spectrometry Laboratory for Biotechnology at North Carolina State University. Partial funding for the facility was obtained from the North Carolina Biotechnology Center and the NSF. We also thank the Oncologic team of Dr Sam Rose (deceased), Dr Henry Rapaport (deceased), Dr Winston Salser, Dr George Mayers, and Dr Chris Knudsen for stimulating discussions.

References

1 A. Jemal, T. Murray, E. Ward, A. Samuels, R. C. Tiwari, A. Ghafoor, E. J. Feuer and M. J. Thun, *CA: Cancer J. Clin.*, 2005, **55**, 10–30.
2 *Cancer Facts and Figure 2007*, American Cancer Society Inc., Atlanta, GA, 2007.
3 (*a*) L. D. Greller, F. L. Tobin and G. Poste, *Invasion Metastasis*, 1996, **16**, 177–208; (*b*) M. E. Lieonart, P. Martin-Duque, R. Sanchez-Prieto, A. Moreno and S. R. Y Cajal, *Histol. Histopath.*, 2000, **15**, 881–898; (*c*) L. Weiss, *Cancer Metastasis Rev.*, 2000, **19**, 345–350; (*d*) H. Kitano, *Nat. Rev. Cancer*, 2004, **4**, 227–235.
4 (*a*) C. V. Ichim and R. A. Wells, *Leukemia Lymphoma*, 2006, **47**, 2017–2027; (*b*) V. S. Donnenberg and A. D. Donnenberg, *J. Clin. Pharmacol.*, 2005, **45**, 872–877.
5 (*a*) K. Sikora, in *Oxford Textbook of Oncology*, ed. M. Peckham, H. Pinedo and U. Veronesi, Oxford University Press, Oxford, 1995, vol. 1, pp. 659–668; (*b*) I. Niculescu-Duvaz and C. J. Springer, *Adv. Drug Delivery Rev.*, 1997, **26**, 151–172; (*c*) R. Duncan, S. Gac-Breton, R. Keane, R. Musila, Y. N. Sat, R. Satchi and F. Searle, *J. Controlled Release*, 2001, **74**, 135–146; (*d*) I. Niculescu-Duvaz and C. J. Springer, *Mol. Biotechnol.*, 2005, **30**, 71–88; (*e*) E. Wagner, R. Kircheis and G. F. Walker, *Biomed. Pharmacother.*, 2004, **58**, 152–161; (*f*) C. P. Leamon and J. A. Reddy, *Adv. Drug Delivery Rev.*, 2004, **56**, 1127–1141; (*g*) D. J. Buchsbaum and D. T. Curiel, *Cancer Biother. Radiopharm.*, 2001, **16**, 275–288.
6 O. C. Boerman, F. G. van Schaijk, W. J. G. Oyen and F. H. M. Corstens, *J. Nucl. Med.*, 2003, **44**, 400–411.
7 D. M. Goldenberg, *Cancer Immunol. Immunother.*, 2003, **52**, 281–296.
8 D. E. Milenic, E. D. Brady and M. W. Brechbiel, *Nat. Rev. Drug Discovery*, 2004, **3**, 488–498.
9 S. V. Govindan, G. L. Griffiths, H. J. Hansen, I. D. Horak and D. M. Goldenberg, *Technol. Cancer Res. Treat.*, 2005, **4**, 375–391.
10 D. M. Goldenberg and R. M. Sharkey, *Quart. J. Nucl. Med. Mol. Imaging*, 2006, **50**, 248–264.

11 C. J. Sunderland, M. Steiert, J. E. Talmadge, A. M. Derfus and S. E. Barry, *Drug Dev. Res.*, 2006, **67**, 70–93.
12 S. Sengupta and R. Sasisekharan, *Br. J. Cancer*, 2007, **96**, 1315–1319.
13 N. H. Patel and M. L. Rothenberg, *Invest. New Drugs*, 1994, **12**, 1–13.
14 S. Rose, *J. Theor. Biol.*, 1998, **195**, 111–128.
15 (*a*) S. Rose, *US Pat.*, 5 816 259, 1998; (*b*) S. Rose, *US Pat.*, 6 080 383, 2000; (*c*) S. Rose, *US Pat.*, 6 468 503 B2, 2002.
16 (*a*) S. Rose, *US Pat. Appl. Publ.*, 20030045458; (*b*) S. Rose, *US Pat. Appl. Publ.*, 20030068382; (*c*) G. L. Mayers, S. Rose and L. Rose, *US Pat. Appl. Publ.*, 20050058652; (*d*) S. Rose, *US Pat. Appl. Publ.*, 20050113290.
17 E. L. Mazzaferri, in *Werner and Ingbar's The Thyroid*, ed. L. E. Braverman and R. D. Utiger, Lippincott-Raven Publishers, Philadelphia, 7th edn, 1996, pp. 922–945.
18 (*a*) J. Nahalka and B. Nidetzky, *Biotechnol. Bioeng.*, 2007, **97**, 454–461; (*b*) S. Dalal, M. Kapoor and M. N. Gupta, *J. Mol. Catal. B: Enzym.*, 2007, **44**, 128–132; (*c*) R. Schoevaart, M. W. Wolbers, M. Golubovic, M. Ottens, A. P. G. Kieboom, F. van Rantwijk, L. A. van der Wielen and R. A. Sheldon, *Biotechnol. Bioeng.*, 2004, **87**, 754–762.
19 G. L. Mayers, *Drug Dev. Res.*, 2006, **67**, 94–106.
20 *Radiotherapy in Practice: Brachytherapy*, ed. P. Hoskin and C. Coyle, Oxford University Press, Oxford, 2005.
21 (*a*) L. A. F. Casciola-Rosen and A. L. Hubbard, *J. Biol. Chem.*, 1991, **266**, 4341–4347; (*b*) R. F. Irvine, N. Hemington and R. M. C. Dawson, *Biochem. J.*, 1978, **176**, 475–484.
22 K. Uchimura, M. Morimoto-Tomita and S. D. Rosen, *Methods Enzymol.*, 2006, **416**, 243–253.
23 M. J. Kuranda and N. N. Aronson, Jr, *J. Biol. Chem.*, 1986, **261**, 5803–5809.
24 G. L. Mayers, D. Lee and H.-L. Chin, *US Pat. Appl. Publ.*, 2006/0018908 A1.
25 J. Carlsson, E. F. Aronsson, S.-O. Hietala, T. Stigbrand and J. Tennvall, *Radiother. Oncol.*, 2003, **66**, 107–117.
26 N.-H. Ho, R. S. Harapanhalli, B. A. Dahman, K. Chen, K. Wang, S. J. Adelstein and A. I. Kassis, *Bioconjugate Chem.*, 2002, **13**, 357–364.
27 K. Wang, A. M. Kirichian, A. F. Al Aowad, S. J. Adelstein and A. I. Kassis, *Bioconjugate Chem.*, 2007, **18**, 754–764.
28 *Histochemistry—Theoretical and Applied*, ed. P. J. Stoward and A. G. E. Pearse, Churchill Livingstone, Edinburgh, 4th edn, 1991, vol. 3.
29 P. Hambright, in *The Porphyrin Handbook*, ed. K. M. Kadish, K. M. Smith and R. Guilard, Academic Press, San Diego, CA, 2000, vol. 3, pp. 129–210.
30 (*a*) Y. Kobuke, *Struct. Bonding*, 2006, **121**, 49–104; (*b*) T. S. Balaban, H. Tamiaki and A. R. Holzwarth, *Top. Curr. Chem.*, 2005, **258**, 1–38; (*c*) T. S. Balaban, *Acc. Chem. Res.*, 2005, **38**, 612–623; (*d*) Z. Wang, C. J. Medforth and J. A. Shelnutt, *J. Am. Chem. Soc.*, 2004, **126**, 15954–15955; (*e*) S.-I. Tamaru, M. Nakamura, M. Takeuchi and S. Shinkai, *Org. Lett.*, 2001, **3**, 3631–3634.
31 P. D. Rao, S. Dhanalekshmi, B. J. Littler and J. S. Lindsey, *J. Org. Chem.*, 2000, **65**, 7323–7344.
32 D. Fan, M. Taniguchi, Z. Yao, S. Dhanalekshmi and J. S. Lindsey, *Tetrahedron*, 2005, **61**, 10291–10303.
33 M. Taniguchi, A. Balakumar, D. Fan, B. E. McDowell and J. S. Lindsey, *J. Porphyrins Phthalocyanines*, 2005, **9**, 554–575.
34 S. H. H. Zaidi, R. M. Fico, Jr. and J. S. Lindsey, *Org. Process Res. Dev.*, 2006, **10**, 118–134.
35 D. K. Dogutan, S. H. H. Zaidi, P. Thamyongkit and J. S. Lindsey, *J. Org. Chem.*, 2007, **72**, 7701–7714.
36 P. Thamyongkit, M. Speckbacher, J. R. Diers, H. L. Kee, C. Kirmaier, D. Holten, D. F. Bocian and J. S. Lindsey, *J. Org. Chem.*, 2004, **69**, 3700–3710.
37 P. Thamyongkit and J. S. Lindsey, *J. Org. Chem.*, 2004, **69**, 5796–5799.
38 K. E. Borbas, P. Mroz, M. R. Hamblin and J. S. Lindsey, *Bioconjugate Chem.*, 2006, **17**, 638–653.
39 (*a*) H. Ali and J. E. van Lier, *Chem. Rev.*, 1999, **99**, 2379–2450; (*b*) R. Fawwaz, P. Bohdiewicz, D. Lavallee, T. Wang, S. Oluwole, J. Newhouse and P. Alderson, *Nucl. Med. Biol.*, 1990, **17** 65–72.
40 A. T. J. Klein, F. Rösch, H. H. Coenen and S. M. Qaim, *Appl. Radiat. Isot.*, 2005, **62**, 711–720.
41 M. C. Crone-Escanye, L. J. Anghileri and J. Robert, *J. Nucl. Med. Allied Sci.*, 1988, **32**, 237–241.
42 (*a*) P. Hambright, J. C. Smart, J. McRae, M. L. Nohr, Y. Yano, P. Chu and A. J. Bearden, *Inorg. Nucl. Chem. Lett.*, 1976, **12**, 217–222; (*b*) L. J. Anghileri, M. Heidbreder and R. Mathes, *Nuklearmedizin*, 1976, **15**, 183–184; (*c*) J. G. McAfee, G. Gagne, G. Subramanian and R. F. Schneider, *J. Nucl. Med.*, 1991, **32**, 2126–2131.
43 R. A. Fawwaz, H. S. Winchell, F. Frye, W. Hemphill and J. H. Lawrence, *J. Nucl. Med.*, 1969, **10**, 581–585.
44 J. C. Roberts, S. L. Newmyer, J. A. Mercer-Smith, S. A. Schreyer and D. K. Lavallee, *Appl. Radiat. Isot.*, 1989, **40**, 775–781.
45 P. Hambright, R. Fawwaz, P. Valk, J. McRae and J. Bearden, *Bioinorg. Chem.*, 1975, **5**, 87–92.
46 (*a*) J. C. Roberts, S. D. Figard, J. A. Mercer-Smith, Z. V. Svitra, W. L. Anderson and D. K. Lavallee, *J. Immunol. Methods*, 1987, **105**, 153–164; (*b*) J. A. Mercer-Smith, J. C. Roberts, S. D. Figard and D. K. Lavallee, in *Targeted Diagnosis and Therapy: Vol. 1. Antibody-Mediated Delivery Systems*, Marcel Dekker, New York, 1988, pp. 317–352.
47 N. Maric, S. M. Chan, P. B. Hoffer and P. Duray, *Nucl. Med. Biol.*, 1988, **15**, 543–551.
48 R. Konirova, M. Ernestova, V. Jedinakova-Krizova and V. Kral, *Czech. J. Phys.*, 2003, **53**, A755–A761.
49 K. Schomäcker, M. I. Gaidouk, V. D. Rumyantseva, T. Fischer, H. Löhr, S. Salditt, S. Liebenhoff and H. Schicha, *Nuklearmedizin*, 1999, **38**, 285–291.
50 (*a*) K. E. Borbas, C. S. M. Ferreira, A. Perkins, J. I. Bruce and S. Missailidis, *Bioconjugate Chem.*, 2007, **18**, 1205–1212; (*b*) S. A. Ali, F. Cesani, M. L. Nusynowitz, E. G. Briscoe, M. E. Shirtliff and J. T. Mader, *J. Nucl. Med.*, 1997, **38**, 1999–2002; (*c*) S. R. Chatterjee, S. Murugesan, J. P. Kamat, S. J. Shetty, T. S. Srivastava, O. P. D. Noronha, A. M. Samuel and T. P. A. Devasagayam, *Arch. Biochem. Biophys.*, 1997 **339**, 242–249; (*d*) S. J. Shetty, S. Murugesan, S. R. Chatterjee, S. Banerjee, T. S. Srivastava, O. P. D. Noronha and A. M. Samuel, *J. Labelled Compd. Radiopharm.*, 1996, **38**, 411–418; (*e*) G. D. Zanelli, I. Bjarnason, T. Smith, J. C. W. Crawley, A. J. Levi and R. I. Copeland, *Nucl. Med. Commun.*, 1986, **7** 17–24.
51 S. Chakraborty, T. Das, S. Banerjee, H. D. Sarma and M. Venkatesh, *Quart. J. Nucl. Med. Mol. Imaging*, 2007, **51**, 16–23.
52 R. A. Fawwaz, W. Hemphill and H. S. Winchell, *J. Nucl. Med.*, 1971, **12**, 231–236.
53 (*a*) N. Foster, D. V. Woo, F. Kaltovich, J. Emrich and C. Ljungquist, *J. Nucl. Med.*, 1985, **26**, 756–760; (*b*) G. D. Robinson, Jr, A. Alavi, R. Vaum and M. Staum, *J. Nucl. Med.*, 1986, **27**, 239–242; (*c*) C. H. Bedel-Cloutour, L. Maneta-Peyret, M. Pereyre and J.-H. Bezian, *J. Immunol. Methods*, 1991, **144**, 35–41; (*d*) M. R. Quastel, A. M. Richter and J. G. Levy, *Br. J. Cancer*, 1990, **62**, 885–890; (*e*) R. T. Palac, L. L. Gray, F. E. Turner, P. H. Brown, M. R. Malinow and H. Demots, *Nucl. Med. Commun.*, 1989, **10**, 841–850.
54 G. D. Zanelli and A. C. Kaelin, *Br. J. Cancer*, 1990, **61**, 687–688.
55 R. R. Kavali, B. C. Lee, B. S. Moon, S. D. Yang, K. S. Chun, C. W. Choi, C.-H. Lee and D. Y. Chi, *J. Labelled Compd. Radiopharm.*, 2005, **48**, 749–758.
56 F. Gao, X. Yan, T. Shakya, O. M. Baettig, S. Ait-Mohand-Brunet, A. M. Berghuis, G. D. Wright and K. Auclair, *J. Med. Chem.*, 2006, **49**, 5273–5281.
57 *Protective Groups in Organic Synthesis*, ed. T. W. Greene and P. G. M. Wuts, John Wiley and Sons, Inc., New York, 3rd edn, 1999.
58 K.-y. Tomizaki, A. B. Lysenko, M. Taniguchi and J. S. Lindsey, *Tetrahedron*, 2004, **60**, 2011–2023.
59 (*a*) J. Lindberg, J. Ekeroth and P. Konradsson, *J. Org. Chem.*, 2002, **67**, 194–199; (*b*) A. Mehta, R. Jaouhari, T. J. Benson and K. T. Douglas, *Tetrahedron Lett.*, 1992, **33**, 5441–5444; (*c*) W. R. Baker, S. Cai, M. Dimitroff, L. Fang, K. K. Huh, D. R. Ryckman, X. Shang, R. M. Shawar and J. H. Therrien, *J. Med. Chem.*, 2004, **47**, 4693–4709.
60 (*a*) M. Cebrat, C. M. Kim, P. R. Thompson, M. Daugherty and P. A. Cole, *Bioorg. Med. Chem.*, 2003, **11**, 3307–3313; (*b*) Y.

Zhang, M. H. Heinsen, M. Kostic, G. M. Pagani, T. V. Riera, I. Perovic, L. Hedstrom, B. B. Snider and T. C. Pochapsky, *Bioorg. Med. Chem.*, 2004, **12**, 3847–3855.
61 (*a*) J. Maung, J. P. Mallari, T. A. Girtsman, L. Y. Wu, J. A. Rowley, N. M. Santiago, A. N. Brunelle and C. E. Berkman, *Bioorg. Med. Chem.*, 2004, **12**, 4969–4979; (*b*) T. Morita, Y. Okamoto and H. Sakurai, *Bull. Chem. Soc. Jpn.*, 1981, **54**, 267–273.
62 (*a*) S. J. Garden, J. C. Torres, S. C. de Souza Melo, A. S. Lima, A. C. Pinto and E. L. S. Lima, *Tetrahedron Lett.*, 2001, **42**, 2089–2092; (*b*) A. R. Hajipour, M. Arbabian and A. E. Ruoho, *J. Org. Chem.*, 2002, **67**, 8622–8624.
63 E. A. Kitas, R. Knorr, A. Trzeciak and W. Bannwarth, *Helv. Chim. Acta*, 1991, **74**, 1314–1328.
64 P. M. Chouinard and P. A. Bartlett, *J. Org. Chem.*, 1986, **51**, 75–78.
65 J. W. Perich, P. F. Alewood and R. B. Johns, *Aust. J. Chem.*, 1991, **44**, 233–252.
66 F. Li, K. Yang, J. S. Tyhonas, K. A. MacCrum and J. S. Lindsey, *Tetrahedron*, 1997, **53**, 12339–12360.
67 S. Saha, A. Bardelli, P. Buckhaults, V. E. Velculescu, C. Rago, B. St. Croix, K. E. Romans, M. A. Choti, C. Lengauer, K. W. Kinzler and B. Vogelstein, *Science*, 2001, **294**, 1343–1346.
68 Z. Yao, *PhD Thesis*, North Carolina State University, 2006.
69 J. Barbet, J.-F. Chatal, F. Gauché and J. Martino, *Eur. J. Nucl. Med. Mol. Imaging*, 2006, **33**, 627–630.
70 N. Srinivasan, C. A. Haney, J. S. Lindsey, W. Zhang and B. T. Chait, *J. Porphyrins Phthalocyanines*, 1999, **3**, 283–291.